Journal Pre-proof

Gold Nanoparticles in Glioma Theranostics

Mohammad Norouzi

PII: S1043-6618(19)32136-X

DOI: https://doi.org/10.1016/j.phrs.2020.104753

Reference: YPHRS 104753

To appear in: *Pharmacological Research*

Received Date: 30 September 2019

Revised Date: 7 March 2020

Accepted Date: 9 March 2020

Please cite this article as: Norouzi M, Gold Nanoparticles in Glioma Theranostics, *Pharmacological Research* (2020), doi: https://doi.org/10.1016/j.phrs.2020.104753

Gold Nanoparticles in Glioma Theranostics

Mohammad Norouzi [1, 2]

1. Department of Biomedical Engineering, University of Manitoba, Winnipeg, MB, Canada
2. Kleysen Institute for Advanced Medicine, Health Sciences Centre, Winnipeg, MB, Canada

Corresponding author: M. Norouzi; norouzim@myumanitoba.ca

Graphical Abstract

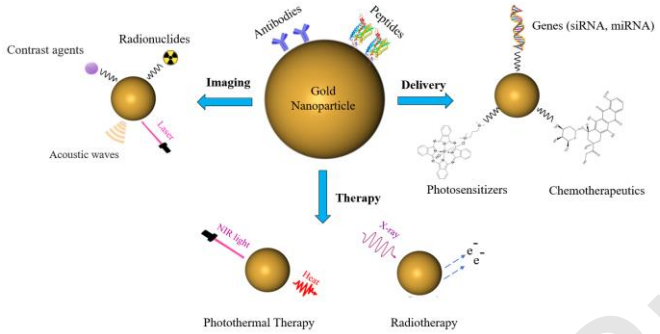

Highlights

- The BBB and the high tumor recurrence rate limit effective treatment of Glioma.
- Gold nanoparticles (AuNPs) exhibit biocompatibility and tunable optical properties.
- AuNP can be an ideal candidate to improve diagnosis and therapy of Glioma.

ABSTRACT

Despite many endeavors to treat malignant gliomas in the last decades, the median survival of patients has not significantly improved. The infiltrative nature of high-grade gliomas and the impermeability of the blood-brain barrier to the most therapeutic agents remain major hurdles, impeding an efficacious treatment. Theranostic platforms bridging diagnosis and therapeutic modalities aim to surmount the

current limitations in diagnosis and therapy of glioma. Gold nanoparticles (AuNPs) due to their biocompatibility and tunable optical properties have widely been utilized for an assortment of theranostic purposes. In this Review, applications of AuNPs as imaging probes, drug/gene delivery systems, radiosensitizers, photothermal transducers, and multimodal theranostic agents in malignant gliomas are discussed. This Review also aims to provide a perspective on cancer theranostic applications of AuNPs in future clinical trials.

Keywords: Gold nanoparticles; Malignant glioma; Glioblastoma; Imaging; Therapy; Theranostic

Contents

1. Introduction

Gliomas are the most common primary tumors of the central nervous system, originated from glial cells (astrocytes, oligodendrocytes or ependymal cells), with an annual incidence of 6.6 per 100,000 individuals in the USA. Gliomas account for 27% of all brain tumors and 80% of all malignant ones [1-3]. According to the World Health Organization (WHO) classification, glioma is divided into four grades. [4]. Glioblastoma multiforme (GBM), a WHO grade IV glioma, is the most prevalent and aggressive form of malignant gliomas characterized by diffuse infiltration of the tumor cells into the brain parenchyma and a high recurrence rate [5-7]. The incidence of GBM is 3.19 per 100,000 persons in the USA [8], and the median survival time of GBM patients who receive the current standard of care is 14.6 months post-diagnosis, while their 5-year survival rate is 9.8% [9-11].

The current standard of care includes surgical resection of the tumor followed by radiation therapy (RT) and adjuvant chemotherapy with temozolomide [12, 13]. However, complete glioma resection is hindered by irregular and indistinct tumor margins, as well as the infiltrative nature of high-grade gliomas invading essential neurological structures [14-16]. After surgery, the invasive cells often form secondary tumors within a few centimeters of the resection site [17, 18]. On the other hand, chemotherapy evidences modest clinical benefits due to the impermeable nature of the blood-brain barrier (BBB) to most of the anticancer agents [19, 20]. The BBB is composed of tight junctions between endothelial cells, surrounding pericytes, as well as the end feet of astrocytes, regulating the passage of substances from the bloodstream into the brain [19, 21-23]. Consequently, a majority of oncotherapeutic and diagnostic agents fail to achieve sufficient concentrations at the tumor vicinity [19, 24, 25]. In addition, the intervention strategies such as temporary disruption of the BBB and direct drug delivery by the intracerebral injection are highly invasive, which cannot be administered for long-term treatments. Moreover, poor solubility

and short half-lives of many therapeutic agents in the blood circulation further limit the chemotherapy efficacy [26, 27]. On the other hand, extensive application of RT is circumscribed by the cumulative dose of radiation that can be safely administered to keep the associated toxicities in the normal surrounding tissues at a tolerable level [28-30].

Hereupon, nanomedicine has emerged as a promising alternative that can surmount the hurdles of the conventional imaging and therapy of gliomas. Amidst the various systems exploited, gold nanoparticles (AuNPs) have attracted much attention by virtue of their biocompatibility, synthetic versatility, unique and tunable optical properties as well as tunable surface functionalities [29, 31, 32]. In addition, nanoparticles have a high surface-area-to-volume ratio, yielding high loading capacity of biomolecules, drugs and imaging contrast agents [33-40]. Thereof, AuNPs have been utilized for a variety of theranostic applications including imaging (e.g. computed tomography, photoacoustic, magnetic resonance and surface-enhanced Raman scattering), delivery (e.g. drugs, proteins, small-interfering RNAs) and therapy (e.g. photothermal therapy, RT) (Fig. 1, Table 1) [29, 41]. Theranostic is generally defined as a platform that bridges the diagnosis and therapeutic modalities [42, 43]. With respect to the imaging-guided therapy, AuNPs can also facilitate delineation of glioma margins with high sensitivity and enable submillimeter spatial resolution rendering microsurgical resection of tumors, along with monitoring drug delivery and treatment progress [19, 44].

Generally, physicochemical properties of AuNPs (like size, shape, surface coating and surface charge) can profoundly affect their biocompatibility, biodistribution as well as functionality [45-48]. In this context,, smaller size AuNPs can typically better cross the BBB through the spaces between astrocyte end-feet and capillary endothelium, extravasate into brain tumor tissue and achieve a more homogeneous intra-tumoral distribution [29, 49]. A comparison between biodistribution of 10 nm, 50 nm, 100 nm and 250 nm AuNPs in healthy rats at 24 h after intravenous (i.v) injection revealed that only 10 nm AuNPs were found ubiquitously distributed in various organs including brain,

whereas the larger particles were only detected in blood, liver and spleen [50]. However, it has been established that as brain tumor progresses, the BBB becomes compromised both structurally and functionally leading to a "leaky" BBB around and within the tumor, whereby the AuNPs in sub-100 nm range can extravasate through these leaky gaps into the tumor tissue and accumulate within the tumor site *via* a mechanism known as the enhanced permeability and retention (EPR) effect [19, 51]. In addition, AuNPs smaller than 10 nm could distribute throughout cytoplasm and nucleus of cancer cells, while larger nanoparticles were found merely in the cytoplasm where they formed aggregates [52]. Moreover, AuNPs smaller than the range of the safe renal clearance (~6 nm) in addition to their higher glioma targeting ability [53], can be excreted rapidly by renal route, whereas larger AuNPs have reported persistence in liver and spleen of mice for up to 6 months [54]. Taken together, a hydrodynamic size range between 10 and 100 nm is required to minimize the fast clearance of nanoparticles and extend their blood half-life [55], while within this size range, smaller nanoparticles are likely to penetrate deeper into the perivascular area of the tumors [56].

Upon i.v. administration, AuNPs are rapidly coated with serum proteins, known as opsonization, to form a protein corona that alters their characteristics and functionality. This non-specific protein binding to the nanoparticle surface is followed by recognition with the mononuclear phagocytic system (MPS), particularly macrophages, and the reticuloendothelial system (RES), such as the liver and spleen, leading to their rapid clearance from the body [29, 49, 57]. To diminish the non-specific protein adsorption, AuNPs are often coated with hydrophilic macromolecules such as poly(ethylene) glycol (PEG) termed as "PEGylation". In fact, PEG coating increases steric hindrance of the AuNPs, prevents their intravascular aggregation and avoids their recognition and clearance by MPS, which ultimately leads to an extended circulation time of the nanoparticles as well as enhanced accumulation in the brain tumor [58-61]. It was also reported that higher PEG modification and smaller particle size can decrease the plasma protein adsorption [62]. Additionally, PEGylated AuNPs can be further functionalized with a variety of targeting moieties such as folate [63], Arg-Gly-Asp (RGD) peptide [64-66], angiopep-2 [67], transferrin (Tf) [68],

epidermal growth factor (EGF) [69, 70], Cetuximab [71], anti-interleukin-13 receptor alpha 2 (anti-IL13Ra2) [72], lactoferrin (Lf) [73], TNYL [74], levodopa (L-dopa) [75], and trans-activator of transcription (TAT) [19] in order to enhance their penetration across the BBB and/or target glioma cells through binding to the receptors overexpressed on these cells. Upon binding the targeting moieties, nanoparticles can be internalized via a *de facto* receptor-mediated endocytosis leading to enhanced cellular uptake and therapeutic efficacy [73].

Hitherto, several AuNPs-based formulations have entered clinical trials for treatment of various cancers, including Aurimmune® (CYT-6091, 27 nm citrate-coated AuNPs bound with thiolated PEG and tumor necrosis factor-α, TNF- α) (ClinicalTrials.gov Identifier: NCT00436410 and NCT00356980), AuroShell® (silica core with a gold shell for photothermal therapy, 150 nm) (NCT01679470, NCT00848042 and NCT02680535) and NU-0129 (siRNA targeting BCL2L12 conjugated to gold nanoparticles, 13 nm) (NCT03020017). This Review focuses on the applications of AuNPs in various imaging and therapeutic modalities of malignant gliomas and this can pave the way for prospective clinical trials of AuNPs in theranostic applications for various cancers.

2. AuNPs Application in Imaging

Efficacious imaging modalities are essential for preoperative planning, intraoperative tumor resection, and therapeutic follow-up in malignant gliomas [14, 19]. A variety of imaging techniques have been exploited to better visualize tumor margins and provide high spatial resolution [76-78]. Photoacoustic (PA) imaging is a relatively new technique that renders high spatial resolution and relatively deep tissue penetration [79]. In PA imaging, tissue is irradiated with a pulsed laser and the light absorption elevates tissue temperature, leading to its thermo-elastic expansion, and consequently propagation of acoustic waves, detected by an ultrasound transducer at the surface of the body [57, 80, 81]. In PA, the first window of near-infrared (NIR, 650-900 nm) wavelength is commonly utilized by virtue of its fair transmissivity in tissues (transmission to a depth of 10 cm in soft tissues and 4 cm in human cadaver

scalp, skull, meninges, and brain) and low absorption by tissue chromophores such as hemoglobin and water [82-85]. Recently, PA imaging in the second window of NIR (1000-1350 nm) has evinced superior imaging ability thanks to a deeper brain skull penetration and a higher signal/background ratio pertained to the low scattering and absorption of the light by biological components [86-88]. AuNPs embedded in the tissue, augment PA signal inasmuch as they convert light to heat more efficiently than the native tissue *per se* does [57, 89, 90].

Raman imaging is another promising and complementary optical imaging technique to discriminate healthy tissue from tumor tissue based on differences in the Raman fingerprints, which can be amplified by the surface-enhanced Raman scattering (SERS) effect of AuNPs accumulated in the tumor tissue [91, 92]. Owing to the unique signature of the SERS spectrum, Raman imaging provides highly specific and sensitive detection of SERS contrast agents especially at the tumor margins, rendering a complete removal of microscopic and invading glioma tumor deposits [14, 93].

Brain magnetic resonance imaging (MRI) is still the golden standard for brain tumor diagnosis, despite the limitations of gadolinium (Gd)-based contrast agents to depict tumor margins. Moreover, intraoperative MRI generally necessitates repeated administration of Gd-chelates, with a short blood half-life that may lead to a surgically induced false-positive contrast enhancement [14]. Compared to Gd alone, Gd-conjugated AuNPs provide a much more concentration of Gd intracellularly and a more lasting enhancement of the brain tumor signals (even detectable after 24 h) resulting in an improved tumor visualization. Therefore, single preoperatively injection of Gd-conjugated AuNPs enables tumor resection by intraoperative MRI, leading to both improved diagnostic accuracy and no toxicity associated with repeated administrations of Gd chelates [14, 94]. Furthermore, Gd-conjugated AuNPs can be utilized as multimodal nanoparticulate contrast agents for a variety of imaging techniques [95-97].

In an importantstudy, unique nanoparticles were developed for triple-modality magnetic resonance imaging–photoacoustic imaging–Raman imaging for both preoperative and intraoperative purposes. For this purpose, Au-silica core-shell nanoparticles were functionalized with a Raman molecular probe and Gd^{3+} ions. Upon i.v. injection of the nanoparticles into orthotopic eGFP+U87MG glioblastoma-bearing mice, the images demonstrated clear visualization of the tumor for all three modalities through the intact skin and skull, in which the MRI contrast-to-noise ratio increased from 2.2 ± 0.3 to 14.0 ± 1.9, the photoacoustic signal enhanced by 75%, from 0.57 ± 0.02 AU to 1.0 ± 0.08 AU and the Raman signal increased from 0 to 1.0 ± 0.09 AU (Fig. 2 A). This signal enhancement lasts 2 h after injection for PA and Raman, and 24 h for MRI [14], whereas the conventional Gd-based contrast agents show rapid clearance within a few minutes post-injection [19]. Of note, the Raman signal provided an accurate delineation of the actual tumor border intraoperatively. In fact, when the tumor resection seemed to be complete by visual inspection, several small foci of residual Raman signals were still being observed in the resection bed, mainly responsible for GBM tumor recurrence after surgical resection (Fig. 2 B) [14].

In a similar study, FAL peptide (Phe-Ala-Leu-Gly-Glu-Ala) as an EGFRvIII targeting ligand, Gd-DTPA chelator as a paramagnetic agent and heptamethine cyanine IR783B as a Raman reporter were decorated on AuNP's surface, for pre-operative MRI and intra-operative surface-enhanced resonance Raman scattering (SERRS) imaging. The T1-weighted-MR signal intensity in the orthotopic U87-EGFRvIII xenograft tumor site increased significantly at 1.0 h post-injection of AuNP-FAL with a greater target to background (T/B) than that of AuNP-PEG (Fig. 3 A). A more distinct tumor margin was delineated at 24 h post-injection by the AuNP-FAL that was well correlated with the tumor defined in histological H&E image (Fig. 3 A & B), indicating the feasibility of imaging-guided tumor resection. Furthermore, the T1 value diminution before and at 24 h post-injection of the nanoprobe, indicated a higher intra-tumoral uptake of AuP-FAL than that of AuP-PEG (Fig. 3 C &D) [98].

Similarly, a radiometal (e.g., ^{64}Cu) can be appended to AuNPs for a multimodal radionuclide-based positron emission tomography (PET) imaging, utilizing the PET's advantage of high sensitivity and quantitative analysis of whole-body [99, 100]. . To integrate PET imaging capability into AuNPs, a radiometal is often coupled to AuNPs via a metal chelator. Be that as it may, attachment of radiometal-chelator complexes faces some challenges of possible detachment of the radiometals as well as alteration of AuNP surface properties. To address these issues, chelator-free ^{64}Cu radiolabeling method via chemically reducing ^{64}Cu on the surface of RGD-PEG-Au nanorods (NRs) (50×15 nm) for PET imaging was exploited. RGD amino acid possesses a high affinity to $\alpha_v\beta_3$ integrin receptors overexpressed on angiogenic endothelial cells and some tumor cells, such as malignant glioma, breast, bladder and prostate cancer cells, rendering it a unique molecular ligand for targeted cancer imaging/therapy [101, 102]. The uptake of RGD-[^{64}Cu]-PEG-AuNRs and [^{64}Cu]-PEG-AuNRs in U87MG subcutaneous tumors were reported 8.37±1.16%ID/g: injected dose per gram of tissue, and 6.19±0.5%ID/g at 24 h post-injection. In spite of the rapid renal clearance of free ^{64}Cu from the body, RGD-[^{64}Cu]-PEG- AuNRs were not excreted by the renal route due to their size, enhancing their blood circulation with a half-life of 17 h [103].

3. AuNPs Application in Chemotherapy

The current standard chemotherapy using temozolomide (TMZ), a DNA-alkylating agent, along with RT can increase the median survival time of GBM patients to 14.6 months, *vs* 12.1 months for patients receiving RT alone [9, 11, 104]. Doxorubicin (DOX) is another chemotherapeutic candidate for brain tumors that is much more potent against glioma cells *in vitro* than TMZ (IC_{50} DOX: 0.1-0.4 µg/ml *vs* IC_{50} TMZ: 24-34 µg/ml on U251 [105]), but it cannot cross the BBB readily, and has a short plasma half-life [19, 106]. cis-Diamminedichloroplatinum (Cisplatin) is another powerful chemotherapeutic against glioma cells, yet it has limited BBB penetration and whose systemically administration is often associated with severe nephrotoxicity and neurotoxicity even at the sub-therapeutic concentrations [107, 108].

An alternative strategy involves incorporation of the chemotherapeutics into small AuNPs that are capable of crossing the BBB. Generally, AuNP-drug conjugates can offer multiple advantages over free drug administration, such as (i) increased bioavailability of the drug by minimizing its inactivation, (ii) enhanced tumor specificity via passive (EPR effect) or active targeting (ligand-mediated), and reduced off-target toxicity (iii) controlled or sustained release of the drug at the tumor site by conjugation on AuNPs via stimuli-sensitive moieties, and (iv) flexibility for multimodal treatments with other therapeutic regimens or imaging techniques in one platform [29, 109-111]. Moreover, drug-loaded AuNPs can overcome efflux transporters present on the BBB, by masking the drugs, leading to enhanced penetration of the chemotherapeutics into the brain [112]. Once the AuNPs reach the brain tumor tissue selectively, the release of the chemotherapeutics can be triggered by the acidic microenvironment or other biological stimuli such as enzyme [113], glutathione [114], or external stimuli such as light or temperature [115, 116]. For example, in pH-sensitive drug release systems, the acidic tumor microenvironment caused by overproduction of lactic acid via fast metabolic rates of cancer cells or the acidic environment of the intracellular compartments like endosomes and lysosomes is exploited [117-119]. Up to now, a variety of AuNP-based drug delivery systems with the capability of crossing the BBB and targeting glioma cells have been developed to deliver chemotherapeutics such as DOX [65, 67, 113] and cisplatin [120, 121].

In one study, DOX was anchored onto AuNPs through hydrazone bond, an acid-responsive linker, then the AuNPs were coated with PEG, and angiopep-2 (An), a ligand that targets low-density lipoprotein receptor-related protein-1 (LRP1) overexpressed on both BBB and glioma cells. The pH-responsive system could release up to 80% of the total anchored DOX at mildly acidic pHs (pH 5 and 6) in two days, while less than 20% of the drug was released at pHs 6.8 and 7.4, at the same period of time. Therefore, once the nanoparticles are taken up by the cells, DOX can be released from AuNPs in the acidic microenvironments and it diffuses into the cytosol and later into the nucleus. Whereas PEG-DOX-AuNPs could only distribute into glioma through the EPR effect, the aniopep-2 could mediate the glioma targeting by specific interaction with LRP1 and thereof a higher distribution of An-PEG-DOX-AuNPs

into glioma cells was observed compared to that of PEG-DOX-AuNPs and free DOX *in vivo*. Correspondingly, orthotopic C6 glioma-bearing mice treated with An-PEG-DOX-AuNPs showed the longest median survival time, which was 2.89 and 1.96-fold longer than that of saline and free DOX, respectively [67]. It is noteworthy to mention that angiopep-2 has generally demonstrated greater transcytosis capacity and parenchymal accumulation than transferrin, lactoferrin, and avidin, and thereof the capability of NPs modified with angiopep-2 to cross the BBB has extensively been exploited [122].

Polymeric micelles self-assembled from amphiphilic block copolymers (e.g. based on PCL-PEG and PLA-PEG) are of great interest for drug delivery because of their advantages such as efficient loading of hydrophobic drugs, antifouling properties, colloidal stability and intrinsic stealth effect. Nonetheless, they have some shortcomings such as low stability *in vivo*, premature drug release, slow and inadequate intracellular drug release, and inefficient tumor cell uptake (due to the effective surface shielding) [123, 124]. To address these issues, stimuli-sensitive micelles which can release anti-cancer drugs in response to an environmental or external stimulus and reduce the stealth effect have been developed [123-125]. For instance, stimuli-sensitive cRGD-directed AuNR/PEG–PCL hybrid nanoparticles (cRGD-HNs) containing DOX were fabricated for targeted chemotherapy of glioblastoma [65]. The release of DOX from cRGD-HNs was triggered by NIR irradiation (808 nm, 0.2 W/cm^2, 5 min) that could increase the cumulative release from 2.0% to 32.6% at 1 h. Furthermore, cRGD-HN-DOX could effectively target human glioma xenografts (Fig. 4 A) and enhanced tumor uptake of DOX released from cRGD-HN by over 3-fold higher than that released from HN (4.06 %ID/g for cRGD-HN compared to 1.24%ID/g for HN). Also, cRGD-HN-DOX demonstrated a reduced accumulation of DOX in lung, liver, spleen, and kidney as compared with HN-DOX (Fig. 4 B & C). Notably, cRGD-HN-DOX+NIR irradiation could completely inhibit tumor growth in U87MG tumor-bearing nude mice, which was more effective than free DOX and non-targeted HN-DOX+NIR (relative tumor volume: 0.98 1.92, 5.26, respectively). The mice treated with cRGD-HN-DOX+NIR all survived over the experimental period of 48 days, as compared to survival of 23 days for those treated with free DOX and 40 days for the cohort treated with HN-DOX+NIR [65]. A similar targeting approach using RRGD, a tandem peptide of RGD and

octarginine, was employed to functionalize gelatin-AuNPs nanoparticles (G-AuNPs) delivering DOX to C6 glioma cells. In this system, gelatin was employed as a substrate of matrix metalloproteinase-2 (MMP-2) that is overexpressed in many kinds of tumors. The G-AuNPs exhibited good tumor retention effect because of their large size, while gelatin was digested by MMP-2 in the tumor and small-sized AuNPs with higher tumor permeability were released [113].

In addition to the passive, and ligand-mediated active targeting of nanoparticles, some other strategies have been recruited to overcome the BBB impermeability and enhance the delivery of nanoparticles into the brain, such as focused ultrasound (FUS), and hyperosmolar disruption of the BBB [126, 127]. Focused ultrasound (FUS) is a physical non-invasive approach that utilizes micro-bubbles circulating in the vasculature, for local and transient disruption of the BBB, thus enhancing the delivery of therapeutic agents into the brain [128]. In this context, PEG-coated Au nanoparticles exhibited over 3-fold higher uptake in right hemispheres upon exposure to FUS (in the presence of circulating MBs), compared to non-sonicated left hemispheres in rat models [129]. Similarly, FUS enhanced the delivery of cisplatin conjugated AuNPs reducing GBM tumor growth *in vivo*. Furthermore, the tissue concentration achieved when using 0.5mg/kg cisplatin in addition to FUS was comparable to the concentration achieved with 5 mg/kg cisplatin in the non-sonicated brain [120]. Moreover, Ye et al. [130] utilized FUS to activate MBs at a targeted site of the brain to increase the local accumulation of intranasally (IN) administered ^{64}Cu-AuNCs that were already beyond the BBB by direct nose-to-brain route. IN administered ^{64}Cu-AuNCs exhibited less accumulation in the blood, lungs, liver, spleen, kidney, and heart vis-à-vis IV injected nanoclusters.

4. AuNPs Application in Radiotherapy

Radiotherapy (RT), alongside surgery and chemotherapy, is the current standard of care for patients with malignant gliomas [9, 11]. The standard radiotherapy regimen for high-grade glioma involves a total dose of 60 Gy in 30–33 fractions of 1.8–2 Gy, or equivalent doses/fractionations [131, 132]. Generally, RT utilizes ionizing radiation to induce double-stranded DNA breaks directly or generate

a cascade of free radicals within cancer cells. Additionally, RT can enhance the permeability of both BBB and blood–brain tumor barrier (BBTB) leading to more efficient delivery of anti-cancer drugs to tumor tissue [30, 133]. Indeed, with the deterioration of brain tumors and gradual impairment of the BBB, the BBTB is formed between brain tumor tissues and microvessels [134-136].

However, since the tissues surrounding tumor are also affected by the radiation, its cumulative dose must be circumscribed to keep toxicities in the normal tissues at a tolerable level that consequently limits the efficacy of RT to kill cancer cells [29, 137]. An alternative approach involves the use of radiosensitizers with high atomic numbers such as iodine, gadolinium and gold to enhance the local dose of radiation [138, 139]. Gold can provide ~2.7 and ~1.66 times higher sensitivity per unit weight than iodine and gadolinium, respectively [139]. In fact, due to the high atomic number (^{79}Au), AuNP absorbs X-rays efficiently and deposits this energy locally, mainly by the emission of photoelectrons and Auger electrons that subsequently can boost the RT dose locally [140]. The effect of AuNPs as a radiosensitizer has been proclaimed in a variety of human cancers, such as head and neck [141], lung [142], prostate [143], and breast [144] cancers.

In this context, PEG-AuNPs (diameter (D)=12 nm, hydrodynamic diameter (D_H)=23 nm) as a radiosensitizer, enhanced DNA damage in both U251 cells (1.7-fold increase) and mouse brain endothelial cells (1.5-fold increase) compared to those irradiated without AuNPs. Through targeting RT to tumor-associated endothelial cells with AuNPs, vasculature fails to deliver nutrients to tumor tissue, resulting in ischemic necrosis and reduced VEGF production. Moreover, mice bearing orthotopic U251 xenografts receiving AuNPs followed by RT showed a median survival time of 28 days *vs* 14 days for mice receiving RT alone. Notably, mice receiving 20 Gy RT prior to AuNPs i.v injection (7 to 14 days before) demonstrated higher gold uptake in the right cerebral hemisphere (3.76±1.9% ID/g) in comparison to the unirradiated control mice [30], indicating that RT can permeabilize BBB and increases the accumulation of AuNPs in tumor tissue particularly in smaller and less disruptive tumors.

Similarly, bovine serum albumin (BSA)-capped AuNPs (D=18 nm, D_H=28 nm) in combination with RT could increase DNA double-strand breaks as well as cell apoptosis in comparison to RT alone in U87 cells. Correspondingly, a maximal tumor growth inhibition was observed in subcutaneous U87-bearing mice receiving AuNPs and RT [28]. As well, AuNPs (D=11.2 nm) injected intravenously into orthopedic Tu2449 glioma-bearing mice could enhance local radiation dose by approximately 300%. The mice receiving AuNPs and radiation (30 Gy RT) demonstrated 50% long-term (>1 year) tumor-free survival, whereas mice receiving radiation alone could not survive more than 150 days [44].

5. AuNPs Application in Photothermal Therapy

Thermotherapy holds great promises as an adjuvant therapy for cancer in two approaches: (i) hyperthermia, in which local/whole-body temperature is elevated to 41–46 °C leading to sensitization, heat-shock response, protein denaturation/folding and apoptosis of cancer cells; (ii) thermal ablation, in which local temperature is elevated over 46 °C leading to necrosis of cancer cells and destruction of the tissue [24, 145, 146]. Photothermal-induced hyperthermia therapy, termed as photothermal therapy (PTT) or plasmonic photothermal therapy relies on the resonant absorption of light by a photothermal transducer (near its plasmon-resonant absorption band) and conversion of the electromagnetic energy into heat as a consequence of electron-phonon interactions [10, 57, 147]. In PTT, typically light in the first NIR window is employed [82-85], and the advantage of the second NIR window in PTT is still controversial [148, 149]. Due to the strong surface plasmon resonance (SPR) effect, the resonant oscillation of free electrons in a conduction band of gold atoms and electric field components induced by incident electromagnetic radiation, several types of Au nanostructures such as AuNPs, Au nanorods (AuNRs) [150, 151], Au nanoshells [152, 153], and Au nanocages [58, 154] have been developed with the SPR peaks tunable in the NIR region, as satisfactory photothermal transducers. Moreover, PTT has shown temporary disruption of the peritumoral BBB in clinical trials on GBM patients with the peak of high permeability within 1–2 weeks after laser ablation and recovery by 4–6 weeks [155], which can enhance drug delivery in into the brain.

Generally, irradiation with a pulsed laser can locally heat AuNRs to high temperatures, inducing melting and re-shaping of the nanorods. However, irradiation with a continuous wave laser light can heat AuNRs continuously without changing the shape of AuNRs. As an alternative, to preclude Au nanostructures from being reshaped upon irradiation and losing their SPR peak, silica-gold nanoshells have been developed [54, 156, 157]. Nanoshells and nanorods are typically more promising candidates for PTT applications compared to their spherical counterparts due to their tunable optical resonance in the NIR region [158, 159]. In the case of nanoshells, the resonance wavelength can be tuned in the NIR region by changing either nanoshell size or the ratio of core/shell radius [78, 158, 160]. AuNRs have two absorption peaks corresponding to the transverse and longitudinal resonances, which can be easily tuned to the NIR region by adjusting the aspect ratio (length/width) [54, 161, 162]. AuroShell® (Nanospectra Biosciences, Inc) is a silica-gold nanoshell coated with PEG that is under clinical trial for PTT of refractory and/or recurrent tumors of head and neck (NCT00848042), as well as prostate cancers (NCT02680535, NCT04240639). The infusion of AuroShell® particles followed by laser irradiation for photothermal ablation of target tissues is called AuroLase® therapy [163, 164]. Also, silica-gold nanoparticles (NANOM-FIM, NCT01270139) have been found safe and clinically efficacious in PTT of atherosclerosis, in a first clinical trial [165, 166]. Still, a successful PTT of tumors depends on both sufficient accumulation of Au nanostructures within the tumor, as well as adequate penetration of the excitation energy, in the clinical practice.

The efficacy of silica-gold nanoshell-mediated PTT was investigated on subcutaneous U373 human glioma-bearing mice. The PEG-coated nanoshell consisted of a spherical dielectric silica core and a thin gold shell with an average particle diameter of 152.0 nm and a SPR peak tuned at 800 nm. Mice received the nanoshells plus laser irradiation exhibited complete tumor regression without sign of recurrence, and four of seven mice survived for the entire 90-day period of study (overall survival = 57%), whereas tumors progressed rapidly in the control group (received laser irradiation alone) and none of the eight mice survived beyond 24 days (mean survival = 13.3 days) [167]. In another study, gold-silica nanoshells

were loaded in macrophages through endocytosis as delivery vehicles exhibiting deep penetration into human glioma spheroids *in vitro*, while complete growth inhibition upon NIR laser irradiation was observed [168, 169]. In fact, circulating macrophages have an intrinsic ability to traverse the intact and compromised BBB, while avoiding interception by the immune system and thereof macrophage-mediated delivery of drugs or nanoparticles has exhibited a great potential in cancer treatment [169, 170]. In a comparative study, anionic-AuNRs were preferred for macrophage-loading due to the higher uptake than neutral-AuNRs and better cell viability than positive-AuNRs. Moreover, anionic-AuNRs loaded in mouse macrophages showed a greater tendency to the hypoxic regions of tumors through macrophages vector as "Trojan Horse", in comparison to passive uptake of anionic-AuNRs in breast tumor-bearing mice [170].

In another study, photothermal efficacy of PEG-Au nanocages (edge length: 48 nm; SPR peak: 800 nm) was examined in subcutaneous U87wtEGFR tumor-bearing mice. Upon irradiation with a continuous-wave diode laser, in nanocage-injected mice, the tumor surface temperature increased rapidly to 50 °C in one minute and began to plateau at 54 °C after 2 min, while in saline-injected mice, the surface temperature remained below 37°C during the entire irradiation (Fig. 5). Moreover, at 24 h post-laser treatment, metabolic activity of tumors in nanocage-treated mice reduced by 70% compared to that of the saline-injected cohort [58]. The unique hollow and porous structure of Au nanocages also make them well suited for encapsulation and controlled release of chemotherapeutics during the PTT.

Rabies virus (RABV), a prototypical neurotropic virus, possesses rabies virus glycoprotein (RVG) that interacts specifically with the nicotinic acetylcholine receptor (AchR) expressed on neuronal cells and therefore enables rabies virus virions to enter the central nervous systems and bypass the BBB. Rabies virus-mimetic silica-coated gold nanorods (length: 120 nm, width: 50 nm, aspect ratio: 2.34 vs live rabies virus's aspect ratio: 2.4) were fabricated and surface-modified with RVG (RVG-PEG-AuNRs@SiO_2) (Fig. 6 A). The RVG-PEG-AuNRs@SiO_2 due to mimicry of the rabies virus in terms of size, shape, and surface properties demonstrated a greater localization in the brain region of mice (Fig. 6

B), with a superior hyperthermal effect in response to NIR laser irradiation compared to their spherical counterpart. With regard to PTT (NIR laser 808 nm, 1.5 W cm^{-2}, 5 min), RVG-PEG-AuNRs@SiO_2 plus NIR could significantly suppress tumor growth or disappeared the tumor in subcutaneous N2a tumor-bearing mice (Fig. 6 C, D & E), whereas plain PEG-AuNRs@SiO_2 barely inhibited the tumor growth. Similarly, orthotopic tumors of mice treated with RVG-PEG-AuNRs@SiO_2 plus NIR were suppressed to a greater extent in comparison to the PEG-AuNRs@SiO_2 plus NIR (Fig. 6 F) [171].

6. AuNPs Application in Photodynamic Therapy

Photodynamic therapy (PDT) is a non-invasive tumor-ablative oncological intervention involving i.v. administration of a tumor-localizing photosensitizer (PS; such as porphyrin, phthalocyanines and bacteriochlorin derivatives) followed by local illumination of tumor with a light of an appropriate wavelength to activate the PS [172-175]. The activated PS transfers its energy to surrounding oxygen, driving generation of highly reactive oxygen species (ROS), such as singlet oxygen ($^1O_2$) that can oxidize key cellular macromolecules leading to tumor cell ablation [172, 176, 177]. It has been acknowledged that PDT drugs can induce cell membrane damage via peroxidation of unsaturated lipids and further damages DNA and cellular organelles such as mitochondria through formation of ROS [70, 178]. Since the majority of PSs are hydrophobic, they lack solubility in physiological solutions and preferentially accumulate in the lipid bilayers of organelle membranes in cancer cells, which consequently hinders their systemic administration. In addition, a relatively long time interval (~1-3 days) between i.v. drug administration and illumination is required to obtain sufficient accumulation of the PSs in the tumor site [178, 179]. Thereof, PEG-AuNPs have been considered as promising and efficient drug delivery platforms for effective PDT, in pre-clinical studies.

Silicon phthalocyanine 4 (Pc 4), a hydrophobic PDT drug, was conjugated non-covalently on PEG-AuNPs (D=5 nm, D_H=38 nm) via N-Au interactions of the terminal amine group on the Pc 4 axial ligand.

Faster diffusion of Pc 4 into the tumor compared to AuNPs indicated that upon accumulation of Pc 4-AuNPs in perivascular space, the Pc 4 was released from the NPs and transported via *de facto* hydrophobic interactions with the lipophilic environment and delivered into the cytoplasm of the tumor cells. Therefore, the AuNPs do not necessarily need to enter the cancer cells in order to deliver the drug. Such a formulation could significantly decrease the time required for the maximum drug accumulation to the target tumor from ~48 h for fee Pc 4, to ≤6 h for Pc 4-AuNPs, prior to irradiation [178, 180].

To improve Pc 4-AuNPs specificity for glioma cells overexpressing transferrin peptide receptors (TfR), transferrin peptide (Tf_{pep}) was conjugated via amide bonds on PEG-AuNPs (D=5.1 nm, D_H=12.3 nm). Tf_{pep}-Pc 4-Au increased drug accumulation by 6 ± 2.2-fold in the brain of orthotopic U87-bearing mice via Tf-containing endosome-mediated internalization, compared to untargeted Pc 4-Au. Upon activation of Pc4 with light at 670 nm, Tf_{pep}-AuNPs-Pc 4 was found more effective than free Pc 4 and AuNPs-Pc 4 at lower concentrations to kill U87 cells *in vitro*, rendering a potential reduction in the current standard therapeutic dose of Pc4 that is 1000 nM [68]. Similarly, AuNPs targeted with epidermal growth factor peptide (EGF_{pep}), enhanced the delivery of Pc 4 to the subcutaneous rat glioma 9L.E29 tumor in mice by 3.3-fold via a ligand-dependent process compared to the non-targeted AuNP-Pc 4. In terms of PDT effect, EGF_{pep} -AuNP-Pc 4 showed the same phototoxic efficiency of free Pc 4, albeit at half the concentration of Pc 4 (0.5×10^{-6} M) on 9L.E29 cells *in vitro*. Although no significant difference was observed *in vivo* on tumor growth inhibition between targeted and non-targeted formulations, it was suggested that the targeted system can be more effective at lower doses of the drug [70]. Later, due to the heterogeneity of overexpressed cell surface receptors within a tumor, AuNPs-Pc4 were conjugated with both EGF_{pep} and Tf_{pep}. The dual-targeted (EGF_{pep}+Tf_{pep})-AuNPs-Pc 4 exhibited significant improvement in drug uptake and cell killing as compared to single-targeted AuNPs pertaining to the synergistic receptor-mediated endocytosis of the ligands [181].

In spite of the therapeutic advantages of PDT, its efficacy can be diminished by the stimulation of an antioxidation balancing system in tumor cells. As a matter of fact, the up-regulation of nuclear factor erythroid 2-related factor 2 (Nrf2) in cancer cells during PDT can induce a significant increment in ABCG2, NQO-1 and HIF-1α expressions, leading to cell resistance to PDT (Fig. 7) [74]. In a comparative study, indocyanine green (ICG) was conjugated on hollow gold nanospheres (HAuNS) modified with TNYL peptide for an active targeting towards EphB4 positive tumors (TNYL-ICG-HAuNS). It was found that the level of Nrf2 was up-regulated upon treatment with both free ICG and TNYL-ICG-HAuNS plus twice laser illuminations due to ROS generation. However, after eight rounds of laser illuminations, in the case of free ICG, due to its instability and easy degradation inside tumor cells, Nrf2 exhibited a gradual decrease to the normal level and the cells were recovered from the oxidative pressure. In the case of TNYL-ICG-HAuNS, whereas they could still produce almost constant ROS in the cells, a significant reduction in HIF-1α level was observed, associated with the activation of cell self-destruction pathway and tumor-killing effect [74].

7. AuNPs Application in Gene Therapy

Gene therapy utilizes nucleic acids to inhibit expression of multiple “undruggable” oncogenes implicated in growth, apoptosis, migration, and invasion of cancer cells [182-184]. The most common types of nucleic acids used for gene therapy are small interfering RNA (siRNA) and micro RNA (miRNA). SiRNA regulates gene expression through degradation of one target messenger RNA (mRNA), while miRNA can regulate multiple genes through either mRNA degradation or blocking translation [185-187]. Despite siRNA which has perfect complementarity to the specific target mRNA, miRNA binds imperfectly to the target mRNA, and this partial complementary binding allows each miRNA to potentially interact with other similar sets in addition to the target mRNA [188, 189].

The translation of gene therapy from the laboratory to the clinic has hitherto been associated with some impediments. (i) the nucleic acids are rapidly cleared from the bloodstream due to their low molecular weight and they are quickly degraded in the presence of nucleases. (ii) they might be entrapped

in endosomes and inadequately penetrate extravascular tumor tissue beyond perivascular regions. (iii) intracellular delivery of these negatively charged molecules necessitates some cationic transfection systems which often cause toxicity. (iv) many of the gene delivery strategies are not cell-specific which may lead to nucleic acid uptake and gene silencing in non-targeted cells [57, 182, 190-192]. To address these issues, AuNPs have been employed as gene delivery systems inasmuch as they offer simple and versatile bioconjugation chemistry while enhancing stability as well as intracellular delivery of the nucleic acids. In addition, PTT can be utilized to facilitate endosomal escape of AuNPs-nucleic acid complexes and trigger gene silencing on demand [193-196].

To date, various nanoparticle-mediated small RNA delivery systems have been developed for glioma gene therapy, targeting a variety of genes such as Bcl2Like12 (Bcl2L12), Luciferase, c-Met, EGFR, miRNA-21, VEGF, Polo-like kinase-1 (PLK1), special AT-rich sequence binding protein 1 (SATB1), and Galectin-1 [197, 198].

Oncoprotein Bcl2L12 is a potent caspase and p53 inhibitor that is overexpressed in GBM specimens [182, 199]. To silence Bcl2L12 overexpression, AuNPs were functionalized covalently with Bcl2L12-specific siRNA duplexes through a thiol-gold bond to develop spherical nucleic acid-nanoparticle conjugates. The AuNPs-siRNA posses an ion cloud associated with a high-density oligonucleotide shell on AuNP core. Therefore, the steric inhibition at the particle surface makes a unique microenvironment inhibiting enzymatic degradation of the nucleic acid, leading to more efficient and enduring gene knockdown in cells and tissues compared to the conventional RNA delivery platforms [182, 200]. Systemically delivered AuNPs-siRNA decreased Bcl2L12 expression in intracerebral GBM, enhanced intratumoral apoptosis, and reduced tumor burden as well as progression in xenografted mice. This strategy can also be applied to sensitize glioma cells toward therapy-induced apoptosis via enhancing effector caspase and p53 activity [182]. NU-0129 is a Bcl2-L12-specific siRNA-coated AuNP that has entered an early phase clinical trial for i.v. injection to treat recurrent GBM or gliosarcoma

(NCT03020017). Intravenous administration of NU-0129 at the dose of 0.04 mg/kg was reported to be tolerated in 8 GBM patients, showing evidence of crossing the BBB and accumulation in the tumor tissue [201].

Polyethyleneimine (PEI)-AuNPs functionalized with RGD was also fabricated as a vector for Bcl-2 siRNA delivery to U87MG cells [202]. It is well established that PEI can protect genes from lysosomal nuclease degradation and furthers endosomal escape to the cytoplasm by virtue of its proton sponge effect [196].

MicroRNA-182 (miR-182) is a tumor suppressor that controls expression and activity of oncogenes deregulated in GBM; i.e., Bcl2L12, and c-Met. Treatment with miR-182 can enhance apoptotic cell death in response to chemotherapeutics such as TMZ and receptor tyrosine kinase (RTK) inhibitors in a Bcl2L12-dependent manner [203-205]. To develop a miRNA-based biotherapeutic gene silencing platform for GBM cells, miR-182-based spherical nucleic acid nanoparticle conjugates (AuNPs-miR-182) were fabricated that could penetrate >90% of glioma cells, diminished Bcl2L12 and c-Met protein levels significantly and enhanced cell apoptosis *in vitro*. Intravenously administrated AuNPs-miR-182 could reduce tumor burden and increased survival of glioma-bearing mice [204].

8. AuNPs Applications in Multimodal Theranostic Regimens

Multimodal theranostic regimens involve the use of (multi-) diagnostic technique and (multi-) therapeutic approach, in order to (i) provide more accurate preoperative and intraoperative imaging, (ii) monitor body response to the treatments, (iii) deliver a variety of therapeutics more efficiently and in a single platform, and (iv) enhance the efficacy of the diagnosis and treatment [14, 78, 206-208].

As an illustration of a multimodal system, AuNRs with the capability of a dual MRI and PA imaging concomitant with an effective PTT was developed for theranostic applications. To this end, AuNRs were coated with poly(N-isopropylacrylamide-comethacrylic acid) (PNIPAAmMA) imparting thermal stability

to the nanoparticles followed by conjugation with magnetic Fe_3O_4 nanoparticles. Using an external magnetic field, the nanorods were guided and concentrated in the tumor sites, and consequently the PA signals were significantly enhanced in subcutaneous C6-tumor-bearing mice. Upon irradiation of the tumor at 808 nm, animals receiving the magnetic NRs showed a profound temperature rise of ΔT=62.8 °C (from 36.3 to 99.1 °C), pertaining to the higher concentration of the magnetic NRs in the tumor vicinity under a magnetic field, while the non-magnetic NRs could only increase the temperature by ΔT=12.1 °C (from 37.3 to 49.4 °C) [209]. Likewise, PEGylated hollow gold nanospheres (AuNS) functionalized with cRGD peptides were fabricated for targeted PA and PTT, by virtue of selective and higher accumulation of cRGD-AuNS in orthotopic U87 glioma (1.12±0.22 %ID/g *vs* 0.38±0.12 %ID/g for non-targeted AuNS) [208].

To amalgamate chemotherapy and MRI imaging regimens, trans-activator of transcription (TAT) peptide-modified AuNPs (D=4.7 nm, D_H=21.4 nm) delivering DOX and Gd^{3+} were synthesized. Targeting AuNPs with TAT could enhance their accumulation in mouse brain tissue by 4.8-fold from 0.6 ± 0.27% ID (AuNPs) to 2.9 ± 0.72% ID (TAT-AuNPs). DOX that was conjugated to the nanoparticles via an acid-labile hydrazone linker was released inside lysosomes (pH = 4.5–6.0), followed by the nuclear translocation of the released DOX. The median overall survival of orthotopic U87 glioma-bearing mice treated with DOX, AuNPs-DOX and TAT-AuNPs-DOX, were reported to be 37.5, 37, and 44 days, respectively, attributed to the improved cellular uptake of DOX. With regard to MRI imaging, Gd^{3+}-conjugated TAT-AuNPs demonstrated a 2.2-fold higher relaxivity and 82-fold increment in Gd^{3+} cellular uptake *in vitro* with a longer retention time *in vivo*, compared to Gd^{3+} chelate [19].

9. Concluding Remarks and Future Perspectives

AuNPs have generally exhibited significant improvements in diagnosis and therapy of a variety of cancers including malignant gliomas, in pre-clinical studies. Overall, AuNPs can (i) provide more accurate and more enduring preoperative and intraoperative multi-modal imaging, enabling complete

resection of migrated tumor cells; (ii) deliver a variety of therapeutics efficiently overcoming the BBB/BBTB; (iii) amalgamate various therapeutic modalities in one platform rendering their synergistic effects; and accordingly (iv) enhance the efficacy of the current therapeutic modalities for gliomas.

AuNPs have also been employed as a platform for immunotherapy of solid tumors, since they *per se* can induce the expression of some proinflammatory cytokines and stimulate the host immune system [210]. Typically, smaller AuNPs (≤15 nm) have shown more immune stimulation compared to their larger counterparts [211, 212]. In terms of AuNP application in immunotherapy, conjugation of recombinant human TNF onto AuNPs resulted in maximal antitumor responses with lower doses of TNF and attenuated off-site toxicity compared to native TNF in colon carcinoma-bearing mice [213]. Later, CYT-6091 (TNF- α bound to the surface of PEGylated 27-nm colloidal AuNPs) was evaluated on 29 patients with solid tumors that could exceed the maximum tolerated dose of TNF by 3-fold, without adverse effects, while CYT-6091 could target the tumor cells [214]. Liu et al., [215] recently reported the synergistic immuno-photothermal therapy using immune checkpoint inhibitor anti-PD-L1 antibody and Au nanostar-mediated PTT in subcutaneous CT-2A glioma-bearing mice. This combinational immuno-photothermal therapy was found significantly effective to reject tumor re-growth after re-challenge in cured mice indicating a generation of memorized antitumor immune response, like an 'anticancer vaccine' effect. The same induced memory immunity effect to prevent glioma recurrence using anti-PD-L1 antibody and DOX- hydroxychloroquine-coated AuNPs was reported in intracranial C6-glioma-bearing mice [216].

As earlier mentioned, some Au-based nanoplatforms have entered clinical trials with some promising results and more pre-clinical and clinical studies are currently undergoing. In this regard, the strengths and limitations of the available studies have been investigated and some suggestions are proposed that may lead to the development of more efficacious Au-based formulations.

In addition to the AuNP's size, surface feature, stability, and interaction with tumor microenvironment, which were discussed, shape is another determining factor that can impact cellular internalization, circulation time and biodistribution of the nanoparticles. However, more comparative studies are still required to investigate the impacts of the shape and other multiple complex factors on pharmacokinetic and therapeutic efficacy of the nanoparticles. For instance, AuNRs were reported to have longer circulation time in the blood, lower uptake by the macrophages and higher accumulation in the tumors, compared to their spherical counterparts [217-219]. In fact, elongated nanoparticles have a higher surface area facilitating a multivalent interaction with target cell receptors *vis-à-vis* the curve shape of spherical particles [219]. Moreover, AuNRs were found to be distributed throughout tumors, whereas Au nanospheres and nanodisks were only observed on the surfaces of tumors [220]. Contrariwise, Black et al., [220] reported that nanospheres showed the best blood circulation, the lowest clearance by the RES, and the highest overall uptake in breast tumors, compared to nanodisks, nanorods, and nanocages. For comparative studies, in addition to surface feature (density of the coatings) and size of different-shaped nanoparticles, weight of the nanoparticles, number of the distributed nanoparticles [218], their blood circulation and clearance time, and their diffusivity need to be considered together.

In view of the uptake of different-shaped nanoparticles by the mononuclear phagocyte system, Au nanoplates with a large contact area with the cells, showed the highest uptake by macrophages *in vitro*, while Au nanorings because of their less contact area with the cell membrane, exhibited a lower level of macrophage uptake. Similarly, macrophage uptake of Au nanospheres, with relatively high surface curvature, was lower than that of Au nanoplates, albeit higher than nanorings, attributed to the smaller contact area of nanorings and nanospheres with the cell membrane compared to nanoplates. Nevertheless, due to the better diffusive properties and smaller encountering resistance, a greater distribution of the nanorings and nanoplates was observed in tumor tissue compared to the nanospheres [221]. In fact, based on the Stokes−Einstein equation, the diffusivity of Au nanoring and nanoplate is almost 50% higher than that of Au nanosphere [221, 222]. AuNRs have also shown higher deposit, permeation and retention in

tumors compared to Au nanoshells [223]. Taken together, it is worth mentioning that AuNRs and other shaped-Au nanoparticles can potentially provide more favorable pharmacokinetic and tumor-homing features than their common spherical counterparts in clinical trials for cancer theranostics.

As mentioned before, drug penetration into glioma cells is hindered by the physiological barriers *i.e.* BBB and BBTB [224, 225]. Although BBB is compromised in the primary tumor site via the EPR effect, it remains mostly intact in regions where tumor cells infiltrate healthy brain parenchyma and therefore drug delivery is impeded to the infiltrated cells that are responsible for tumor recurrence after surgical resection [73, 226]. Furthermore, the increased interstitial fluid pressure is liable to oppose the passive drug diffusion into the brain tumor tissue [227]. Remarkably, although passive targeting via the EPR effect has been shown in preclinical models, this effect has not been satisfactory in humans [228], and it is impacted by tumor's type, size and heterogeneity, disease stage as well as interpatient variability [229]. Functionalizing AuNPs with targeting moieties not only can increase their uptake and internalization via receptor-mediated endocytosis, but also can be utilized to target tumor cells, migrating from the primary tumor sites as well as metastatic tumors, through recognition of the tumor-specific receptors on the cancer cells [64, 73]. Moreover, due to the heterogeneity of overexpressed cell surface receptors within a tumor, multi-targeted nanoparticles have exhibited superiority over the single-targeted counterparts [181].

With regard to animal studies, due to the difficulty of orthotopic glioma model establishment, a subcutaneous glioma tumor model is regularly studied. Nevertheless, the subcutaneous tumor model underestimates (i) the BBB impermeability, (ii) the lower permeability of the BBTB compared to the blood-tumor barrier (BTB) in peripheral tissues, and (iii) the high interstitial pressure in brain tumors [230, 231]. More importantly, a majority of researches merely rely on animal models, howbeit rodents do not necessarily mimic humans with respect to tumor's growth rate, size relative to body mass, and microenvironment. Last but not least, the long-term retention of AuNPs especially in the spleen, liver and even skin, and their whole-body clearance need to be further studied. Therefore, future pilot studies in

clinical research are warranted to appraise the efficacy of Au-based nanoplatforms in theranostic of various cancers including glioma [228, 232].

Declarations of interest

Declarations of interest: none.

References

[1] K. Grauwet, E.A. Chiocca, Glioma and microglia, a double entendre, Nature immunology 17(11) (2016) 1240.
[2] M. Norouzi, B. Nazari, D.W. Miller, Electrospun-based systems in cancer therapy, Electrospun Materials for Tissue Engineering and Biomedical Applications, Elsevier2017, pp. 337-356.
[3] I. Appolloni, M. Barilari, S. Caviglia, E. Gambini, E. Reisoli, P. Malatesta, A cadherin switch underlies malignancy in high-grade gliomas, Oncogene 34(15) (2015) 1991.
[4] V.P. Ferrer, V. Moura Neto, R. Mentlein, Glioma infiltration and extracellular matrix: key players and modulators, Glia 66(8) (2018) 1542-1565.
[5] Y. Liu, J. Lu, Z. Zhang, L. Zhu, S. Dong, G. Guo, R. Li, Y. Nan, K. Yu, Y. Zhong, Amlexanox, a selective inhibitor of IKBKE, generates anti-tumoral effects by disrupting the Hippo pathway in human glioblastoma cell lines, Cell death & disease 8(8) (2017) e3022.
[6] C. Ricard, F. Stanchi, G. Rougon, F. Debarbieux, An orthotopic glioblastoma mouse model maintaining brain parenchymal physical constraints and suitable for intravital two-photon microscopy, Journal of visualized experiments : JoVE (86). doi(86) (2014) 10.3791/51108.
[7] E.A. Maher, R.M. Bachoo, Glioblastoma, Rosenberg's Molecular and Genetic Basis of Neurological and Psychiatric Disease (Fifth Edition), Elsevier2015, pp. 909-917.
[8] K.E. Parrish, J.N. Sarkaria, W.F. Elmquist, Improving drug delivery to primary and metastatic brain tumors: strategies to overcome the blood–brain barrier, Clinical Pharmacology & Therapeutics 97(4) (2015) 336-346.
[9] R. Stupp, W.P. Mason, M.J. Van Den Bent, M. Weller, B. Fisher, M.J.B. Taphoorn, K. Belanger, A.A. Brandes, C. Marosi, U. Bogdahn, Radiotherapy plus concomitant and adjuvant temozolomide for glioblastoma, New England Journal of Medicine 352(10) (2005) 987-996.
[10] J.M. Heffernan, J.B. McNamara, S. Borwege, B.L. Vernon, N. Sanai, S. Mehta, R.W. Sirianni, PNIPAAm-co-Jeffamine®(PNJ) scaffolds as in vitro models for niche enrichment of glioblastoma stem-like cells, Biomaterials 143 (2017) 149-158.
[11] R. Stupp, M.E. Hegi, W.P. Mason, M.J. van den Bent, M.J.B. Taphoorn, R.C. Janzer, S.K. Ludwin, A. Allgeier, B. Fisher, K. Belanger, Effects of radiotherapy with concomitant and adjuvant temozolomide versus radiotherapy alone on survival in glioblastoma in a randomised phase III study: 5-year analysis of the EORTC-NCIC trial, The lancet oncology 10(5) (2009) 459-466.
[12] L. Hathout, B. Ellingson, W. Pope, Modeling the efficacy of the extent of surgical resection in the setting of radiation therapy for glioblastoma, Cancer science 107(8) (2016) 1110-1116.
[13] L. Schiefer, M. Visweswaran, V. Perumal, F. Arfuso, D. Groth, P. Newsholme, S. Warrier, A. Dharmarajan, Epigenetic regulation of the secreted frizzled-related protein family in human glioblastoma multiforme, Cancer gene therapy 21(7) (2014) 297.
[14] M.F. Kircher, A. De La Zerda, J.V. Jokerst, C.L. Zavaleta, P.J. Kempen, E. Mittra, K. Pitter, R. Huang, C. Campos, F. Habte, A brain tumor molecular imaging strategy using a new triple-modality MRI-photoacoustic-Raman nanoparticle, Nature medicine 18(5) (2012) 829.
[15] H. Karabeber, R. Huang, P. Iacono, J.M. Samii, K. Pitter, E.C. Holland, M.F. Kircher, Guiding brain tumor resection using surface-enhanced Raman scattering nanoparticles and a hand-held Raman scanner, Acs Nano 8(10) (2014) 9755-9766.
[16] R. Ankri, A. Ashkenazy, Y. Milstein, Y. Brami, A. Olshinka, N. Goldenberg-Cohen, A. Popovtzer, D. Fixler, A. Hirshberg, Gold nanorods based air scanning electron microscopy and diffusion reflection imaging for mapping tumor margins in squamous cell carcinoma, ACS nano 10(2) (2016) 2349-2356.

[17] D. Huang, C. Lin, X. Wen, S. Gu, P. Zhao, A Potential Nanofiber Membrane Device for Filling Surgical Residual Cavity to Prevent Glioma Recurrence and Improve Local Neural Tissue Reconstruction, PloS one 11(8) (2016) e0161435.
[18] Y.-Y. Tseng, Y.-C. Wang, C.-H. Su, T.-C. Yang, T.-M. Chang, Y.-C. Kau, S.-J. Liu, Concurrent delivery of carmustine, irinotecan, and cisplatin to the cerebral cavity using biodegradable nanofibers: in vitro and in vivo studies, Colloids and Surfaces B: Biointerfaces 134 (2015) 254-261.
[19] Y. Cheng, Q. Dai, R.A. Morshed, X. Fan, M.L. Wegscheid, D.A. Wainwright, Y. Han, L. Zhang, B. Auffinger, A.L. Tobias, Blood-brain barrier permeable gold nanoparticles: an efficient delivery platform for enhanced malignant glioma therapy and imaging, Small 10(24) (2014) 5137-5150.
[20] G.D. Kenny, A.S. Bienemann, A.D. Tagalakis, J.A. Pugh, K. Welser, F. Campbell, A.B. Tabor, H.C. Hailes, S.S. Gill, M.F. Lythgoe, Multifunctional receptor-targeted nanocomplexes for the delivery of therapeutic nucleic acids to the brain, Biomaterials 34(36) (2013) 9190-9200.
[21] L.Y. Di Marco, A. Venneri, E. Farkas, P.C. Evans, A. Marzo, A.F. Frangi, Vascular dysfunction in the pathogenesis of Alzheimer's disease—a review of endothelium-mediated mechanisms and ensuing vicious circles, Neurobiology of disease 82 (2015) 593-606.
[22] M. Tavazoie, L. Van der Veken, V. Silva-Vargas, M. Louissaint, L. Colonna, B. Zaidi, J.M. Garcia-Verdugo, F. Doetsch, A specialized vascular niche for adult neural stem cells, Cell stem cell 3(3) (2008) 279-288.
[23] H.-G. Bernstein, G. Hölzl, H. Dobrowolny, J. Hildebrandt, K. Trübner, M. Krohn, B. Bogerts, J. Pahnke, Vascular and extravascular distribution of the ATP-binding cassette transporters ABCB1 and ABCC1 in aged human brain and pituitary, Mechanisms of ageing and development 141 (2014) 12-21.
[24] M. Norouzi, B. Nazari, D.W. Miller, Injectable hydrogel-based drug delivery systems for local cancer therapy, Drug discovery today (2016).
[25] M. Norouzi, Z. Abdali, S. Liu, D.W. Miller, Salinomycin-loaded Nanofibers for Glioblastoma Therapy, Scientific reports 8(1) (2018) 9377.
[26] F. Sousa, S. Mandal, C. Garrovo, A. Astolfo, A. Bonifacio, D. Latawiec, R.H. Menk, F. Arfelli, S. Huewel, G. Legname, Functionalized gold nanoparticles: a detailed in vivo multimodal microscopic brain distribution study, Nanoscale 2(12) (2010) 2826-2834.
[27] Y.-Y. Tseng, J.-Y. Liao, W.-A. Chen, Y.-C. Kao, S.-J. Liu, Sustainable release of carmustine from biodegradable poly [(D, L)-lactide-co-glycolide] nanofibrous membranes in the cerebral cavity: in vitro and in vivo studies, Expert opinion on drug delivery 10(7) (2013) 879-888.
[28] N. Chen, W. Yang, Y. Bao, H. Xu, S. Qin, Y. Tu, BSA capped Au nanoparticle as an efficient sensitizer for glioblastoma tumor radiation therapy, RSC Advances 5(51) (2015) 40514-40520.
[29] S. Her, D.A. Jaffray, C. Allen, Gold nanoparticles for applications in cancer radiotherapy: Mechanisms and recent advancements, Advanced Drug Delivery Reviews 109 (2017) 84-101.
[30] D.Y. Joh, L. Sun, M. Stangl, A. Al Zaki, S. Murty, P.P. Santoiemma, J.J. Davis, B.C. Baumann, M. Alonso-Basanta, D. Bhang, Selective targeting of brain tumors with gold nanoparticle-induced radiosensitization, PloS one 8(4) (2013) e62425.
[31] N. Ma, P. Liu, N. He, N. Gu, F.-G. Wu, Z. Chen, Action of Gold Nanospikes-Based Nanoradiosensitizers: Cellular Internalization, Radiotherapy, and Autophagy, ACS applied materials & interfaces 9(37) (2017) 31526-31542.
[32] A. Cantelli, G. Battistelli, G. Guidetti, J. Manzi, M. Di Giosia, M. Montalti, Luminescent gold nanoclusters as biocompatible probes for optical imaging and theranostics, Dyes and Pigments 135 (2016) 64-79.
[33] S.-m. Park, A. Aalipour, O. Vermesh, J.H. Yu, S.S. Gambhir, Towards clinically translatable in vivo nanodiagnostics, Nature Reviews Materials 2(5) (2017) 17014.
[34] D. Bobo, K.J. Robinson, J. Islam, K.J. Thurecht, S.R. Corrie, Nanoparticle-based medicines: a review of FDA-approved materials and clinical trials to date, Pharmaceutical research 33(10) (2016) 2373-2387.

[35] A.H. Hekmati, M. Norouzi, Electrospun scaffolds for cardiac tissue engineering, Electrospun Materials for Tissue Engineering and Biomedical Applications, Elsevier2017, pp. 289-297.
[36] M. Norouzi, I. Shabani, H.H. Ahvaz, M. Soleimani, PLGA/gelatin hybrid nanofibrous scaffolds encapsulating EGF for skin regeneration, Journal of biomedical materials research Part A 103(7) (2015) 2225-2235.
[37] M. Norouzi, M. Soleimani, I. Shabani, F. Atyabi, H.H. Ahvaz, A. Rashidi, Protein encapsulated in electrospun nanofibrous scaffolds for tissue engineering applications, Polymer International 62(8) (2013) 1250-1256.
[38] S. Vakilian, M. Norouzi, M. Soufi-Zomorrod, I. Shabani, S. Hosseinzadeh, M. Soleimani, L. inermis-loaded nanofibrous scaffolds for wound dressing applications, Tissue and Cell (2018).
[39] M. Norouzi, M. Soleimani, EGF-Loaded Nanofibers for Skin Tissue Engineering, (2016).
[40] O. Mirdailami, M. Soleimani, R. Dinarvand, M.R. Khoshayand, M. Norouzi, A. Hajarizadeh, M. Dodel, F. Atyabi, Controlled release of rhEGF and rhbFGF from electrospun scaffolds for skin regeneration, Journal of Biomedical Materials Research Part A 103(10) (2015) 3374-3385.
[41] M.E. Gindy, R.K. Prud'homme, Multifunctional nanoparticles for imaging, delivery and targeting in cancer therapy, Expert opinion on drug delivery 6(8) (2009) 865-878.
[42] J. Hu, X. Zhu, H. Li, Z. Zhao, X. Chi, G. Huang, D. Huang, G. Liu, X. Wang, J. Gao, Theranostic Au cubic nano-aggregates as potential photoacoustic contrast and photothermal therapeutic agents, Theranostics 4(5) (2014) 534-545.
[43] X. Zhu, X. Chi, J. Chen, L. Wang, X. Wang, Z. Chen, J. Gao, Real-time monitoring in vivo behaviors of theranostic nanoparticles by contrast-enhanced T1 imaging, Analytical Chemistry 87(17) (2015) 8941-8948.
[44] J.F. Hainfeld, H.M. Smilowitz, M.J. O'Connor, F.A. Dilmanian, D.N. Slatkin, Gold nanoparticle imaging and radiotherapy of brain tumors in mice, Nanomedicine 8(10) (2013) 1601-1609.
[45] N.P. Truong, M.R. Whittaker, C.W. Mak, T.P. Davis, The importance of nanoparticle shape in cancer drug delivery, Expert opinion on drug delivery 12(1) (2015) 129-142.
[46] M.S. Verma, P.Z. Chen, L. Jones, F.X. Gu, "Chemical nose" for the visual identification of emerging ocular pathogens using gold nanostars, Biosensors and Bioelectronics 61 (2014) 386-390.
[47] N.N.M. Adnan, Y.Y. Cheng, N.M.N. Ong, T.T. Kamaruddin, E. Rozlan, T.W. Schmidt, H.T.T. Duong, C. Boyer, Effect of gold nanoparticle shapes for phototherapy and drug delivery, Polymer Chemistry 7(16) (2016) 2888-2903.
[48] P.M. Tiwari, S.S. Bawage, S.R. Singh, Gold nanoparticles and their applications in photomedicine, diagnosis and therapy, Applications of Nanoscience in Photomedicine, Elsevier2015, pp. 249-266.
[49] A. Kumar, X. Zhang, X.-J. Liang, Gold nanoparticles: emerging paradigm for targeted drug delivery system, Biotechnology Advances 31(5) (2013) 593-606.
[50] W.H. De Jong, W.I. Hagens, P. Krystek, M.C. Burger, A.J.A.M. Sips, R.E. Geertsma, Particle size-dependent organ distribution of gold nanoparticles after intravenous administration, Biomaterials 29(12) (2008) 1912-1919.
[51] T.-T. Zhang, W. Li, G. Meng, P. Wang, W. Liao, Strategies for transporting nanoparticles across the blood–brain barrier, Biomaterials science 4(2) (2016) 219-229.
[52] K. Huang, H. Ma, J. Liu, S. Huo, A. Kumar, T. Wei, X. Zhang, S. Jin, Y. Gan, P.C. Wang, Size-dependent localization and penetration of ultrasmall gold nanoparticles in cancer cells, multicellular spheroids, and tumors in vivo, ACS nano 6(5) (2012) 4483-4493.
[53] C. Peng, X. Gao, J. Xu, B. Du, X. Ning, S. Tang, R.M. Bachoo, M. Yu, W.-P. Ge, J. Zheng, Targeting orthotopic gliomas with renal-clearable luminescent gold nanoparticles, Nano research 10(4) (2017) 1366-1376.

[54] L.C. Kennedy, L.R. Bickford, N.A. Lewinski, A.J. Coughlin, Y. Hu, E.S. Day, J.L. West, R.A. Drezek, A new era for cancer treatment: gold-nanoparticle-mediated thermal therapies, Small 7(2) (2011) 169-183.
[55] A.K. Gupta, M. Gupta, Synthesis and surface engineering of iron oxide nanoparticles for biomedical applications, biomaterials 26(18) (2005) 3995-4021.
[56] S.D. Perrault, C. Walkey, T. Jennings, H.C. Fischer, W.C. Chan, Mediating tumor targeting efficiency of nanoparticles through design, Nano letters 9(5) (2009) 1909-1915.
[57] R.S. Riley, E.S. Day, Gold nanoparticle-mediated photothermal therapy: applications and opportunities for multimodal cancer treatment, Wiley Interdisciplinary Reviews: Nanomedicine and Nanobiotechnology 9(4) (2017).
[58] J. Chen, C. Glaus, R. Laforest, Q. Zhang, M. Yang, M. Gidding, M.J. Welch, Y. Xia, Gold nanocages as photothermal transducers for cancer treatment, Small 6(7) (2010) 811-817.
[59] J.R. Melamed, R.S. Riley, D.M. Valcourt, E.S. Day, Using gold nanoparticles to disrupt the tumor microenvironment: an emerging therapeutic strategy, ACS nano 10(12) (2016) 10631-10635.
[60] J.V. Jokerst, T. Lobovkina, R.N. Zare, S.S. Gambhir, Nanoparticle PEGylation for imaging and therapy, Nanomedicine 6(4) (2011) 715-728.
[61] J. Lipka, M. Semmler-Behnke, R.A. Sperling, A. Wenk, S. Takenaka, C. Schleh, T. Kissel, W.J. Parak, W.G. Kreyling, Biodistribution of PEG-modified gold nanoparticles following intratracheal instillation and intravenous injection, Biomaterials 31(25) (2010) 6574-6581.
[62] W. Xiao, J. Xiong, S. Zhang, Y. Xiong, H. Zhang, H. Gao, Influence of ligands property and particle size of gold nanoparticles on the protein adsorption and corresponding targeting ability, International journal of pharmaceutics (2018).
[63] J. Guo, M. Schlich, J.F. Cryan, C.M. O'Driscoll, Targeted Drug Delivery via Folate Receptors for the Treatment of Brain Cancer: Can the Promise Deliver?, Journal of pharmaceutical sciences 106(12) (2017) 3413-3420.
[64] J. Choi, J. Yang, J. Park, E. Kim, J.S. Suh, Y.M. Huh, S. Haam, Specific near-IR absorption imaging of glioblastomas using integrin-targeting gold nanorods, Advanced Functional Materials 21(6) (2011) 1082-1088.
[65] Y. Zhong, C. Wang, R. Cheng, L. Cheng, F. Meng, Z. Liu, Z. Zhong, cRGD-directed, NIR-responsive and robust AuNR/PEG–PCL hybrid nanoparticles for targeted chemotherapy of glioblastoma in vivo, Journal of Controlled Release 195 (2014) 63-71.
[66] B. Albertini, V. Mathieu, N. Iraci, M. Van Woensel, A. Schoubben, A. Donnadio, S.M. Greco, M. Ricci, A. Temperini, P. Blasi, Tumor targeting by peptide decorated gold nanoparticles, Molecular pharmaceutics (2019).
[67] S. Ruan, M. Yuan, L. Zhang, G. Hu, J. Chen, X. Cun, Q. Zhang, Y. Yang, Q. He, H. Gao, Tumor microenvironment sensitive doxorubicin delivery and release to glioma using angiopep-2 decorated gold nanoparticles, Biomaterials 37 (2015) 425-435.
[68] S. Dixit, T. Novak, K. Miller, Y. Zhu, M.E. Kenney, A.-M. Broome, Transferrin receptor-targeted theranostic gold nanoparticles for photosensitizer delivery in brain tumors, Nanoscale 7(5) (2015) 1782-1790.
[69] Q. Feng, Y. Shen, Y. Fu, M.E. Muroski, P. Zhang, Q. Wang, C. Xu, M.S. Lesniak, G. Li, Y. Cheng, Self-assembly of gold nanoparticles shows microenvironment-mediated dynamic switching and enhanced brain tumor targeting, Theranostics 7(7) (2017) 1875.
[70] J.D. Meyers, Y. Cheng, A.M. Broome, R.S. Agnes, M.D. Schluchter, S. Margevicius, X. Wang, M.E. Kenney, C. Burda, J.P. Basilion, Peptide-Targeted Gold Nanoparticles for Photodynamic Therapy of Brain Cancer, Particle & Particle Systems Characterization 32(4) (2015) 448-457.
[71] N. Groysbeck, A. Stoessel, M. Donzeau, E.C. da Silva, M. Lehmann, J.-M. Strub, S. Cianferani, K. Dembélé, G. Zuber, Synthesis and biological evaluation of 2.4 nm thiolate-protected gold nanoparticles

conjugated to Cetuximab for targeting glioblastoma cancer cells via the EGFR, Nanotechnology 30(18) (2019) 184005.
[72] R.J. Bernardi, A.R. Lowery, P.A. Thompson, S.M. Blaney, J.L. West, Immunonanoshells for targeted photothermal ablation in medulloblastoma and glioma: an in vitro evaluation using human cell lines, Journal of neuro-oncology 86(2) (2008) 165-172.
[73] A.S. Wadajkar, J.G. Dancy, D.S. Hersh, P. Anastasiadis, N.L. Tran, G.F. Woodworth, J.A. Winkles, A.J. Kim, Tumor-targeted nanotherapeutics: overcoming treatment barriers for glioblastoma, Wiley Interdisciplinary Reviews: Nanomedicine and Nanobiotechnology 9(4) (2017).
[74] W. Li, X. Guo, F. Kong, H. Zhang, L. Luo, Q. Li, C. Zhu, J. Yang, Y. Du, J. You, Overcoming photodynamic resistance and tumor targeting dual-therapy mediated by indocyanine green conjugated gold nanospheres, Journal of Controlled Release 258 (2017) 171-181.
[75] L. Nair, R. Nair, S. Shenoy, A. Thekkuveettil, R. Jayasree, Blood brain barrier permeable gold nanocluster for targeted brain imaging and therapy: an in vitro and in vivo study, Journal of Materials Chemistry B 5(42) (2017) 8314-8321.
[76] W. Shang, C. Zeng, Y. Du, H. Hui, X. Liang, C. Chi, K. Wang, Z. Wang, J. Tian, Core–shell gold Nanorod@ metal–organic framework nanoprobes for multimodality diagnosis of glioma, Advanced Materials 29(3) (2017) 1604381.
[77] C. Cilliers, I. Nessler, N. Christodolu, G.M. Thurber, Tracking antibody distribution with near-infrared fluorescent dyes: impact of dye structure and degree of labeling on plasma clearance, Molecular pharmaceutics 14(5) (2017) 1623-1633.
[78] Y. Cheng, R.A. Morshed, B. Auffinger, A.L. Tobias, M.S. Lesniak, Multifunctional nanoparticles for brain tumor imaging and therapy, Advanced Drug Delivery Reviews 66 (2014) 42-57.
[79] M. Roach, J.L. Alberini, A.P. Pecking, A. Testori, F. Verrecchia, J. Soteldo, U. Ganswindt, J.L. Joyal, J.W. Babich, R.S. Witte, Diagnostic and therapeutic imaging for cancer: therapeutic considerations and future directions, Journal of surgical oncology 103(6) (2011) 587-601.
[80] M.K.A. Singh, M. Jaeger, M. Frenz, W. Steenbergen, In vivo demonstration of reflection artifact reduction in photoacoustic imaging using synthetic aperture photoacoustic-guided focused ultrasound (PAFUSion), Biomedical optics express 7(8) (2016) 2955-2972.
[81] T. Mitcham, K. Dextraze, H. Taghavi, M. Melancon, R. Bouchard, Photoacoustic imaging driven by an interstitial irradiation source, Photoacoustics 3(2) (2015) 45-54.
[82] C.E. Tedford, S. DeLapp, S. Jacques, J. Anders, Quantitative analysis of transcranial and intraparenchymal light penetration in human cadaver brain tissue, Lasers in surgery and medicine 47(4) (2015) 312-322.
[83] L. An, Y. Wang, Q. Tian, S. Yang, Small Gold Nanorods: Recent Advances in Synthesis, Biological Imaging, and Cancer Therapy, Materials 10(12) (2017) 1372.
[84] A. Agarwal, M.A. Mackey, M.A. El-Sayed, R.V. Bellamkonda, Remote triggered release of doxorubicin in tumors by synergistic application of thermosensitive liposomes and gold nanorods, ACS nano 5(6) (2011) 4919-4926.
[85] M. Yu, F. Guo, F. Tan, N. Li, Dual-targeting nanocarrier system based on thermosensitive liposomes and gold nanorods for cancer thermo-chemotherapy, Journal of Controlled Release 215 (2015) 91-100.
[86] Z. Cao, L. Feng, G. Zhang, J. Wang, S. Shen, D. Li, X. Yang, Semiconducting polymer-based nanoparticles with strong absorbance in NIR-II window for in vivo photothermal therapy and photoacoustic imaging, Biomaterials 155 (2018) 103-111.
[87] B. Guo, Z. Sheng, D. Hu, X. Lin, S. Xu, C. Liu, H. Zheng, B. Liu, Biocompatible conjugated polymer nanoparticles for highly efficient photoacoustic imaging of orthotopic brain tumors in the second near-infrared window, Materials Horizons 4(6) (2017) 1151-1156.
[88] A.M. Smith, M.C. Mancini, S. Nie, Bioimaging: second window for in vivo imaging, Nature nanotechnology 4(11) (2009) 710.

[89] D. Pan, M. Pramanik, A. Senpan, S. Ghosh, S.A. Wickline, L.V. Wang, G.M. Lanza, Near infrared photoacoustic detection of sentinel lymph nodes with gold nanobeacons, Biomaterials 31(14) (2010) 4088-4093.
[90] W. Li, X. Chen, Gold nanoparticles for photoacoustic imaging, Nanomedicine 10(2) (2015) 299-320.
[91] S. Jeong, Y.-i. Kim, H. Kang, G. Kim, M.G. Cha, H. Chang, K.O. Jung, Y.-H. Kim, B.-H. Jun, Y.-S. Lee, Fluorescence-Raman dual modal endoscopic system for multiplexed molecular diagnostics, Scientific reports 5 (2015) 9455.
[92] S. Harmsen, M.A. Wall, R. Huang, M.F. Kircher, Cancer imaging using surface-enhanced resonance Raman scattering nanoparticles, Nature protocols 12(7) (2017) 1400.
[93] B.A. Kairdolf, A. Bouras, M. Kaluzova, A.K. Sharma, M.D. Wang, C.G. Hadjipanayis, S. Nie, Intraoperative spectroscopy with ultrahigh sensitivity for image-guided surgery of malignant brain tumors, Analytical Chemistry 88(1) (2015) 858-867.
[94] A. Meola, J. Rao, N. Chaudhary, M. Sharma, S.D. Chang, Gold nanoparticles for brain tumor imaging: a systematic review, Frontiers in neurology 9 (2018).
[95] J.H. Mokkath, U. Schwingenschlögl, Gd doped Au nanoclusters: Molecular magnets with novel properties, Chemical Physics Letters 592 (2014) 217-221.
[96] Y. Cao, L. Xu, Y. Kuang, D. Xiong, R. Pei, Gadolinium-based nanoscale MRI contrast agents for tumor imaging, Journal of Materials Chemistry B 5(19) (2017) 3431-3461.
[97] C. Tian, L. Zhu, F. Lin, S.G. Boyes, Poly (acrylic acid) bridged gadolinium metal–organic framework–gold nanoparticle composites as contrast agents for computed tomography and magnetic resonance bimodal imaging, ACS applied materials & interfaces 7(32) (2015) 17765-17775.
[98] Q. Yue, X. Gao, Y. Yu, Y. Li, W. Hua, K. Fan, R. Zhang, J. Qian, L. Chen, C. Li, An EGFRvIII targeted dual-modal gold nanoprobe for imaging-guided brain tumor surgery, Nanoscale 9(23) (2017) 7930-7940.
[99] Y. Zhao, D. Sultan, L. Detering, S. Cho, G. Sun, R. Pierce, K.L. Wooley, Y. Liu, Copper-64-Alloyed Gold Nanoparticles for Cancer Imaging: Improved Radiolabel Stability and Diagnostic Accuracy, Angewandte Chemie International Edition 53(1) (2014) 156-159.
[100] Y. Zhao, L. Detering, D. Sultan, M.L. Cooper, M. You, S. Cho, S.L. Meier, H. Luehmann, G. Sun, M. Rettig, Gold Nanoclusters Doped with 64Cu for CXCR4 Positron Emission Tomography Imaging of Breast Cancer and Metastasis, ACS nano 10(6) (2016) 5959-5970.
[101] M.E. Davis, Z. Chen, D.M. Shin, Nanoparticle therapeutics: an emerging treatment modality for cancer, Nanoscience And Technology: A Collection of Reviews from Nature Journals, World Scientific2010, pp. 239-250.
[102] Y. Zhong, F. Meng, C. Deng, Z. Zhong, Ligand-directed active tumor-targeting polymeric nanoparticles for cancer chemotherapy, Biomacromolecules 15(6) (2014) 1955-1969.
[103] X. Sun, X. Huang, X. Yan, Y. Wang, J. Guo, O. Jacobson, D. Liu, L.P. Szajek, W. Zhu, G. Niu, Chelator-free 64Cu-integrated gold nanomaterials for positron emission tomography imaging guided photothermal cancer therapy, ACS nano 8(8) (2014) 8438-8446.
[104] D. Nanegrungsunk, W. Onchan, N. Chattipakorn, S.C. Chattipakorn, Current evidence of temozolomide and bevacizumab in treatment of gliomas, Neurological research 37(2) (2015) 167-183.
[105] C.o.C.L.I. capital Ka, O.Y. Klyuchivska, I.I. Grytsyna, N. Finiuk, R.R. Panchuk, M.O. Starykovych, L. Lehka, R.B. Lesyk, U.B.S. Zsmall i, R.S. Stoika, Differential pro-apoptotic effects of synthetic 4-thiazolidinone derivative Les-3288, doxorubicin and temozolomide in human glioma U251 cells, Croatian medical journal 58(2) (2017) 150-159.
[106] J. Park, Y. Zhang, N. Vykhodtseva, F.A. Jolesz, N.J. McDannold, The kinetics of blood brain barrier permeability and targeted doxorubicin delivery into brain induced by focused ultrasound, Journal of Controlled Release 162(1) (2012) 134-142.

[107] H. Uchino, Y. Matsumura, T. Negishi, F. Koizumi, T. Hayashi, T. Honda, N. Nishiyama, K. Kataoka, S. Naito, T. Kakizoe, Cisplatin-incorporating polymeric micelles (NC-6004) can reduce nephrotoxicity and neurotoxicity of cisplatin in rats, British journal of cancer 93(6) (2005) 678.
[108] J. Rousseau, R.F. Barth, M. Fernandez, J.-F. Adam, J. Balosso, F. Estève, H. Elleaume, Efficacy of intracerebral delivery of cisplatin in combination with photon irradiation for treatment of brain tumors, Journal of neuro-oncology 98(3) (2010) 287-295.
[109] O.S. Muddineti, B. Ghosh, S. Biswas, Current trends in using polymer coated gold nanoparticles for cancer therapy, International journal of pharmaceutics 484(1-2) (2015) 252-267.
[110] L. Vigderman, E.R. Zubarev, Therapeutic platforms based on gold nanoparticles and their covalent conjugates with drug molecules, Advanced Drug Delivery Reviews 65(5) (2013) 663-676.
[111] R. Cao-Milán, L.M. Liz-Marzán, Gold nanoparticle conjugates: recent advances toward clinical applications, Expert opinion on drug delivery 11(5) (2014) 741-752.
[112] H. Liu, J. Zhang, X. Chen, X.-S. Du, J.-L. Zhang, G. Liu, W.-G. Zhang, Application of iron oxide nanoparticles in glioma imaging and therapy: from bench to bedside, Nanoscale 8(15) (2016) 7808-7826.
[113] S. Ruan, Q. He, H. Gao, Matrix metalloproteinase triggered size-shrinkable gelatin-gold fabricated nanoparticles for tumor microenvironment sensitive penetration and diagnosis of glioma, Nanoscale 7(21) (2015) 9487-9496.
[114] X. Wang, X. Cai, J. Hu, N. Shao, F. Wang, Q. Zhang, J. Xiao, Y. Cheng, Glutathione-triggered “off–on” release of anticancer drugs from dendrimer-encapsulated gold nanoparticles, Journal of the American Chemical Society 135(26) (2013) 9805-9810.
[115] J. You, G. Zhang, C. Li, Exceptionally high payload of doxorubicin in hollow gold nanospheres for near-infrared light-triggered drug release, ACS nano 4(2) (2010) 1033-1041.
[116] Y. Ma, X. Liang, S. Tong, G. Bao, Q. Ren, Z. Dai, Gold Nanoshell Nanomicelles for Potential Magnetic Resonance Imaging, Light-Triggered Drug Release, and Photothermal Therapy, Advanced functional materials 23(7) (2013) 815-822.
[117] J. Gautier, E. Allard-Vannier, E. Munnier, M. Soucé, I. Chourpa, Recent advances in theranostic nanocarriers of doxorubicin based on iron oxide and gold nanoparticles, Journal of Controlled Release 169(1) (2013) 48-61.
[118] F. Wang, Y.-C. Wang, S. Dou, M.-H. Xiong, T.-M. Sun, J. Wang, Doxorubicin-tethered responsive gold nanoparticles facilitate intracellular drug delivery for overcoming multidrug resistance in cancer cells, ACS nano 5(5) (2011) 3679-3692.
[119] J. Liu, Y. Huang, A. Kumar, A. Tan, S. Jin, A. Mozhi, X.-J. Liang, pH-Sensitive nano-systems for drug delivery in cancer therapy, Biotechnology Advances 32(4) (2014) 693-710.
[120] D. Coluccia, C.A. Figueiredo, M.Y. Wu, A.N. Riemenschneider, R. Diaz, A. Luck, C. Smith, S. Das, C. Ackerley, M. O’Reilly, Enhancing glioblastoma treatment using cisplatin-gold-nanoparticle conjugates and targeted delivery with magnetic resonance-guided focused ultrasound, Nanomedicine: Nanotechnology, Biology and Medicine 14(4) (2018) 1137-1148.
[121] S. Setua, M. Ouberai, S.G. Piccirillo, C. Watts, M. Welland, Cisplatin-tethered gold nanospheres for multimodal chemo-radiotherapy of glioblastoma, Nanoscale 6(18) (2014) 10865-10873.
[122] S. Huang, J. Li, L. Han, S. Liu, H. Ma, R. Huang, C. Jiang, Dual targeting effect of Angiopep-2-modified, DNA-loaded nanoparticles for glioma, Biomaterials 32(28) (2011) 6832-6838.
[123] C. Deng, Y. Jiang, R. Cheng, F. Meng, Z. Zhong, Biodegradable polymeric micelles for targeted and controlled anticancer drug delivery: promises, progress and prospects, Nano Today 7(5) (2012) 467-480.
[124] H.M. Aliabadi, A. Lavasanifar, Polymeric micelles for drug delivery, Expert opinion on drug delivery 3(1) (2006) 139-162.
[125] H. Wei, S.-X. Cheng, X.-Z. Zhang, R.-X. Zhuo, Thermo-sensitive polymeric micelles based on poly (N-isopropylacrylamide) as drug carriers, Progress in Polymer Science 34(9) (2009) 893-910.

[126] O. Maksimenko, J. Malinovskaya, E. Shipulo, N. Osipova, V. Razzhivina, D. Arantseva, O. Yarovaya, U. Mostovaya, A. Khalansky, V. Fedoseeva, Doxorubicin-loaded PLGA nanoparticles for the chemotherapy of glioblastoma: Towards the pharmaceutical development, International journal of pharmaceutics 572 (2019) 118733.
[127] R.J. Piper, M.A. Hughes, C.M. Moran, J. Kandasamy, Focused ultrasound as a non-invasive intervention for neurological disease: a review, British journal of neurosurgery 30(3) (2016) 286-293.
[128] M.G.Z. Ghali, V.M. Srinivasan, P. Kan, Focused ultrasound-mediated blood brain barrier disruption in the enhancement of delivery of brain tumor therapies, World neurosurgery (2019).
[129] A.B. Etame, R.J. Diaz, M.A. O'Reilly, C.A. Smith, T.G. Mainprize, K. Hynynen, J.T. Rutka, Enhanced delivery of gold nanoparticles with therapeutic potential into the brain using MRI-guided focused ultrasound, Nanomedicine: Nanotechnology, Biology and Medicine 8(7) (2012) 1133-1142.
[130] D. Ye, X. Zhang, Y. Yue, R. Raliya, P. Biswas, S. Taylor, Y.-c. Tai, J.B. Rubin, Y. Liu, H. Chen, Focused ultrasound combined with microbubble-mediated intranasal delivery of gold nanoclusters to the brain, Journal of controlled release 286 (2018) 145-153.
[131] R. Stupp, M. Brada, M.J. Van Den Bent, J.C. Tonn, G. Pentheroudakis, High-grade glioma: ESMO Clinical Practice Guidelines for diagnosis, treatment and follow-up, Annals of oncology 25(suppl_3) (2014) iii93-iii101.
[132] R. Stupp, J.C. Tonn, M. Brada, G. Pentheroudakis, E.G.W. Group, High-grade malignant glioma: ESMO Clinical Practice Guidelines for diagnosis, treatment and follow-up, Annals of oncology 21(suppl_5) (2010) v190-v193.
[133] C. Wang, H. Nie, Y. Li, G. Liu, X. Wang, S. Xing, L. Zhang, X. Chen, Y. Chen, Y. Li, The study of the relation of DNA repair pathway genes SNPs and the sensitivity to radiotherapy and chemotherapy of NSCLC, Scientific reports 6 (2016) 26526.
[134] C. Chen, Z. Duan, Y. Yuan, R. Li, L. Pang, J. Liang, X. Xu, J. Wang, Peptide-22 and cyclic RGD functionalized liposomes for glioma targeting drug delivery overcoming BBB and BBTB, ACS applied materials & interfaces 9(7) (2017) 5864-5873.
[135] J. Mao, D. Ran, C. Xie, Q. Shen, S. Wang, W. Lu, EGFR/EGFRvIII Dual-Targeting Peptide-Mediated Drug Delivery for Enhanced Glioma Therapy, ACS applied materials & interfaces 9(29) (2017) 24462-24475.
[136] X. Wei, X. Chen, M. Ying, W. Lu, Brain tumor-targeted drug delivery strategies, Acta Pharmaceutica Sinica B 4(3) (2014) 193-201.
[137] M.D. Hasselle, D.J. Haraf, K.E. Rusthoven, D.W. Golden, R. Salgia, V.M. Villaflor, N. Shah, P.C. Hoffman, S.J. Chmura, P.P. Connell, Hypofractionated image-guided radiation therapy for patients with limited volume metastatic non-small cell lung cancer, Journal of thoracic oncology 7(2) (2012) 376-381.
[138] M. Edouard, D. Broggio, Y. Prezado, F. Estève, H. Elleaume, J.-F. Adam, Treatment plans optimization for contrast-enhanced synchrotron stereotactic radiotherapy, Medical physics 37(6Part1) (2010) 2445-2456.
[139] N. Goswami, Z. Luo, X. Yuan, D.T. Leong, J. Xie, Engineering gold-based radiosensitizers for cancer radiotherapy, Materials Horizons 4(5) (2017) 817-831.
[140] W. Ngwa, R. Kumar, S. Sridhar, H. Korideck, P. Zygmanski, R.A. Cormack, R. Berbeco, G.M. Makrigiorgos, Targeted radiotherapy with gold nanoparticles: current status and future perspectives, Nanomedicine 9(7) (2014) 1063-1082.
[141] A. Popovtzer, A. Mizrachi, M. Motiei, D. Bragilovski, L. Lubimov, M. Levi, O. Hilly, I. Ben-Aharon, R. Popovtzer, Actively targeted gold nanoparticles as novel radiosensitizer agents: an in vivo head and neck cancer model, Nanoscale 8(5) (2016) 2678-2685.
[142] C. Wang, X. Li, Y. Wang, Z. Liu, L. Fu, L. Hu, Enhancement of radiation effect and increase of apoptosis in lung cancer cells by thio-glucose-bound gold nanoparticles at megavoltage radiation energies, Journal of nanoparticle research 15(5) (2013) 1642.

[143] X. Zhang, J.Z. Xing, J. Chen, L. Ko, J. Amanie, S. Gulavita, N. Pervez, D. Yee, R. Moore, W. Roa, Enhanced radiation sensitivity in prostate cancer by gold-nanoparticles, Clinical & Investigative Medicine 31(3) (2008) 160-167.
[144] N. Chattopadhyay, Z. Cai, Y.L. Kwon, E. Lechtman, J.-P. Pignol, R.M. Reilly, Molecularly targeted gold nanoparticles enhance the radiation response of breast cancer cells and tumor xenografts to X-radiation, Breast cancer research and treatment 137(1) (2013) 81-91.
[145] V.F. Cardoso, A. Francesko, C. Ribeiro, M. Bañobre-López, P. Martins, S. Lanceros-Mendez, Advances in magnetic nanoparticles for biomedical applications, Advanced healthcare materials 7(5) (2018) 1700845.
[146] M.S. Mohamed, S. Veeranarayanan, T. Maekawa, D.S. Kumar, External stimulus responsive inorganic nanomaterials for cancer theranostics, Advanced Drug Delivery Reviews (2018).
[147] F.C.P. Masim, H.-L. Liu, M. Porta, T. Yonezawa, A. Balčytis, S. Juodkazis, W.-H. Hsu, K. Hatanaka, Enhanced photoacoustics from gold nano-colloidal suspensions under femtosecond laser excitation, Optics Express 24(13) (2016) 14781-14792.
[148] P. Vijayaraghavan, C.H. Liu, R. Vankayala, C.S. Chiang, K.C. Hwang, Designing Multi-Branched Gold Nanoechinus for NIR Light Activated Dual Modal Photodynamic and Photothermal Therapy in the Second Biological Window, Advanced materials 26(39) (2014) 6689-6695.
[149] M.-F. Tsai, S.-H.G. Chang, F.-Y. Cheng, V. Shanmugam, Y.-S. Cheng, C.-H. Su, C.-S. Yeh, Au nanorod design as light-absorber in the first and second biological near-infrared windows for in vivo photothermal therapy, ACS nano 7(6) (2013) 5330-5342.
[150] X. Huang, I.H. El-Sayed, W. Qian, M.A. El-Sayed, Cancer cell imaging and photothermal therapy in the near-infrared region by using gold nanorods, Journal of the American Chemical Society 128(6) (2006) 2115-2120.
[151] W.S. Kuo, C.N. Chang, Y.T. Chang, M.H. Yang, Y.H. Chien, S.J. Chen, C.S. Yeh, Gold nanorods in photodynamic therapy, as hyperthermia agents, and in near-infrared optical imaging, Angewandte Chemie 122(15) (2010) 2771-2775.
[152] B.G. Prevo, S.A. Esakoff, A. Mikhailovsky, J.A. Zasadzinski, Scalable Routes to Gold Nanoshells with Tunable Sizes and Response to Near-Infrared Pulsed-Laser Irradiation, Small 4(8) (2008) 1183-1195.
[153] X. Ji, R. Shao, A.M. Elliott, R.J. Stafford, E. Esparza-Coss, J.A. Bankson, G. Liang, Z.-P. Luo, K. Park, J.T. Markert, Bifunctional gold nanoshells with a superparamagnetic iron oxide− silica core suitable for both MR imaging and photothermal therapy, The Journal of Physical Chemistry C 111(17) (2007) 6245-6251.
[154] S.E. Skrabalak, J. Chen, L. Au, X. Lu, X. Li, Y. Xia, Gold nanocages for biomedical applications, Advanced Materials 19(20) (2007) 3177-3184.
[155] E.C. Leuthardt, C. Duan, M.J. Kim, J.L. Campian, A.H. Kim, M.M. Miller-Thomas, J.S. Shimony, D.D. Tran, Hyperthermic laser ablation of recurrent glioblastoma leads to temporary disruption of the peritumoral blood brain barrier, PLoS One 11(2) (2016).
[156] A.B. Taylor, A.M. Siddiquee, J.W.M. Chon, Below melting point photothermal reshaping of single gold nanorods driven by surface diffusion, Acs Nano 8(12) (2014) 12071-12079.
[157] H. Takahashi, T. Niidome, A. Nariai, Y. Niidome, S. Yamada, Photothermal reshaping of gold nanorods prevents further cell death, Nanotechnology 17(17) (2006) 4431.
[158] P.K. Jain, K.S. Lee, I.H. El-Sayed, M.A. El-Sayed, Calculated absorption and scattering properties of gold nanoparticles of different size, shape, and composition: applications in biological imaging and biomedicine, The journal of physical chemistry B 110(14) (2006) 7238-7248.
[159] M.P. Melancon, W. Lu, C. Li, Gold-based magneto/optical nanostructures: challenges for in vivo applications in cancer diagnostics and therapy, MRS bulletin 34(6) (2009) 415-421.

[160] K. Jiang, D.A. Smith, A. Pinchuk, Size-dependent photothermal conversion efficiencies of plasmonically heated gold nanoparticles, The Journal of Physical Chemistry C 117(51) (2013) 27073-27080.
[161] H. Li, G. Zheng, L. Xu, W. Su, Influence of amount of CTAB and ascorbic acid concentration on localized surface plasmon resonance property of gold nanorod, Optik-International Journal for Light and Electron Optics 125(9) (2014) 2044-2047.
[162] Y. Bai, C. Gao, Y. Yin, Fully alloyed Ag/Au nanorods with tunable surface plasmon resonance and high chemical stability, Nanoscale 9(39) (2017) 14875-14880.
[163] E.-M. Kim, H.-J. Jeong, Current status and future direction of nanomedicine: focus on advanced biological and medical applications, Nuclear medicine and molecular imaging 51(2) (2017) 106-117.
[164] F. Chen, W. Cai, Nanomedicine for targeted photothermal cancer therapy: where are we now?, Nanomedicine 10(1) (2015) 1-3.
[165] A.N. Kharlamov, A.E. Tyurnina, V.S. Veselova, O.P. Kovtun, V.Y. Shur, J.L. Gabinsky, Silica–gold nanoparticles for atheroprotective management of plaques: results of the NANOM-FIM trial, Nanoscale 7(17) (2015) 8003-8015.
[166] A.N. Kharlamov, J.A. Feinstein, J.A. Cramer, J.A. Boothroyd, E.V. Shishkina, V. Shur, Plasmonic photothermal therapy of atherosclerosis with nanoparticles: long-term outcomes and safety in NANOM-FIM trial, Future cardiology 13(4) (2017) 345-363.
[167] E.S. Day, P.A. Thompson, L. Zhang, N.A. Lewinski, N. Ahmed, R.A. Drezek, S.M. Blaney, J.L. West, Nanoshell-mediated photothermal therapy improves survival in a murine glioma model, Journal of neuro-oncology 104(1) (2011) 55-63.
[168] S.J. Madsen, S.-K. Baek, A.R. Makkouk, T. Krasieva, H. Hirschberg, Macrophages as cell-based delivery systems for nanoshells in photothermal therapy, Annals of Biomedical Engineering 40(2) (2012) 507-515.
[169] S.-K. Baek, A.R. Makkouk, T. Krasieva, C.-H. Sun, S.J. Madsen, H. Hirschberg, Photothermal treatment of glioma; an in vitro study of macrophage-mediated delivery of gold nanoshells, Journal of neuro-oncology 104(2) (2011) 439-448.
[170] L. An, Y. Wang, J. Lin, Q. Tian, Y. Xie, J. Hu, S. Yang, Macrophages-Mediated Delivery of Small Gold Nanorods for Tumor Hypoxia Photoacoustic Imaging and Enhanced Photothermal Therapy, ACS applied materials & interfaces 11(17) (2019) 15251-15261.
[171] C. Lee, H.S. Hwang, S. Lee, B. Kim, J.O. Kim, K.T. Oh, E.S. Lee, H.G. Choi, Y.S. Youn, Rabies virus-inspired silica-coated gold nanorods as a photothermal therapeutic platform for treating brain tumors, Advanced Materials 29(13) (2017) 1605563.
[172] S.S. Lucky, K.C. Soo, Y. Zhang, Nanoparticles in photodynamic therapy, Chemical reviews 115(4) (2015) 1990-2042.
[173] H. Zhu, Y. Fang, Q. Miao, X. Qi, D. Ding, P. Chen, K. Pu, Regulating Near-Infrared Photodynamic Properties of Semiconducting Polymer Nanotheranostics for Optimized Cancer Therapy, ACS nano 11(9) (2017) 8998-9009.
[174] J. Ge, M. Lan, B. Zhou, W. Liu, L. Guo, H. Wang, Q. Jia, G. Niu, X. Huang, H. Zhou, A graphene quantum dot photodynamic therapy agent with high singlet oxygen generation, Nature communications 5 (2014) 4596.
[175] Y. He, A. del Valle, Y. Qian, Y.-F. Huang, Near infrared light-mediated enhancement of reactive oxygen species generation through electron transfer from graphene oxide to iron hydroxide/oxide, Nanoscale 9(4) (2017) 1559-1566.
[176] Y. Liu, K. Ma, T. Jiao, R. Xing, G. Shen, X. Yan, Water-insoluble photosensitizer nanocolloids stabilized by supramolecular interfacial assembly towards photodynamic therapy, Scientific reports 7 (2017) 42978.

[177] J. Wang, Y. Li, R. Mao, Y. Wang, X. Yan, J. Liu, Persistent luminescent nanoparticles as energy mediators for enhanced photodynamic therapy with fractionated irradiation, Journal of Materials Chemistry B 5(29) (2017) 5793-5805.
[178] Y. Cheng, J.D. Meyers, A.-M. Broome, M.E. Kenney, J.P. Basilion, C. Burda, Deep penetration of a PDT drug into tumors by noncovalent drug-gold nanoparticle conjugates, Journal of the American Chemical Society 133(8) (2011) 2583-2591.
[179] N.F. Gamaleia, I.O. Shton, Gold mining for PDT: Great expectations from tiny nanoparticles, Photodiagnosis and photodynamic therapy 12(2) (2015) 221-231.
[180] Y. Cheng, A.C. Samia, J.D. Meyers, I. Panagopoulos, B. Fei, C. Burda, Highly efficient drug delivery with gold nanoparticle vectors for in vivo photodynamic therapy of cancer, Journal of the American Chemical Society 130(32) (2008) 10643-10647.
[181] S. Dixit, K. Miller, Y. Zhu, E. McKinnon, T. Novak, M.E. Kenney, A.-M. Broome, Dual receptor-targeted theranostic nanoparticles for localized delivery and activation of photodynamic therapy drug in glioblastomas, Molecular pharmaceutics 12(9) (2015) 3250-3260.
[182] S.A. Jensen, E.S. Day, C.H. Ko, L.A. Hurley, J.P. Luciano, F.M. Kouri, T.J. Merkel, A.J. Luthi, P.C. Patel, J.I. Cutler, W.L. Daniel, A.W. Scott, M.W. Rotz, T.J. Meade, D.A. Giljohann, C.A. Mirkin, A.H. Stegh, Spherical nucleic acid nanoparticle conjugates as an RNAi-based therapy for glioblastoma, Science translational medicine 5(209) (2013) 209ra152.
[183] J. Luo, CRISPR/Cas9: from genome engineering to cancer drug discovery, Trends in cancer 2(6) (2016) 313-324.
[184] J. Ning, S.D. Rabkin, Current Status of Gene Therapy for Brain Tumors, Translating Gene Therapy to the Clinic, Elsevier2015, pp. 305-323.
[185] Y. Shu, F. Pi, A. Sharma, M. Rajabi, F. Haque, D. Shu, M. Leggas, B.M. Evers, P. Guo, Stable RNA nanoparticles as potential new generation drugs for cancer therapy, Advanced Drug Delivery Reviews 66 (2014) 74-89.
[186] K. Felekkis, E. Touvana, C. Stefanou, C. Deltas, microRNAs: a newly described class of encoded molecules that play a role in health and disease, Hippokratia 14(4) (2010) 236-240.
[187] S.K. Shenouda, S.K. Alahari, MicroRNA function in cancer: oncogene or a tumor suppressor?, Cancer and metastasis reviews 28(3-4) (2009) 369.
[188] J. Wang, Z. Lu, M.G. Wientjes, J.L.S. Au, Delivery of siRNA therapeutics: barriers and carriers, The AAPS journal 12(4) (2010) 492-503.
[189] M. Muthiah, I.-K. Park, C.-S. Cho, Nanoparticle-mediated delivery of therapeutic genes: focus on miRNA therapeutics, Expert opinion on drug delivery 10(9) (2013) 1259-1273.
[190] A.K. Varkouhi, M. Scholte, G. Storm, H.J. Haisma, Endosomal escape pathways for delivery of biologicals, Journal of Controlled Release 151(3) (2011) 220-228.
[191] Z.-W. Wu, C.-T. Chien, C.-Y. Liu, J.-Y. Yan, S.-Y. Lin, Recent progress in copolymer-mediated siRNA delivery, Journal of drug targeting 20(7) (2012) 551-560.
[192] N.S. Gandhi, R.K. Tekade, M.B. Chougule, Nanocarrier mediated delivery of siRNA/miRNA in combination with chemotherapeutic agents for cancer therapy: current progress and advances, Journal of Controlled Release 194 (2014) 238-256.
[193] A. Barhoumi, R. Huschka, R. Bardhan, M.W. Knight, N.J. Halas, Light-induced release of DNA from plasmon-resonant nanoparticles: Towards light-controlled gene therapy, Chemical Physics Letters 482(4-6) (2009) 171-179.
[194] W. Lu, G. Zhang, R. Zhang, L.G. Flores, 2nd, Q. Huang, J.G. Gelovani, C. Li, Tumor site-specific silencing of NF-kappaB p65 by targeted hollow gold nanosphere-mediated photothermal transfection, Cancer research 70(8) (2010) 3177-3188.
[195] G.B. Braun, A. Pallaoro, G. Wu, D. Missirlis, J.A. Zasadzinski, M. Tirrell, N.O. Reich, Laser-activated gene silencing via gold nanoshell− siRNA conjugates, Acs Nano 3(7) (2009) 2007-2015.

[196] F. Wang, W. Zhang, Y. Shen, Q. Huang, D. Zhou, S. Guo, Efficient RNA delivery by integrin-targeted glutathione responsive polyethyleneimine capped gold nanorods, Acta biomaterialia 23 (2015) 136-146.
[197] A. Aigner, D. Kögel, Nanoparticle/siRNA-based therapy strategies in glioma: which nanoparticles, which siRNAs?, Nanomedicine 13(1) (2018) 89-103.
[198] P. Játiva, V. Ceña, Use of nanoparticles for glioblastoma treatment: a new approach, Nanomedicine 12(20) (2017) 2533-2554.
[199] T.L. Sita, F.M. Kouri, L.A. Hurley, T.J. Merkel, A. Chalastanis, J.L. May, S.T. Ghelfi, L.E. Cole, T.C. Cayton, S.N. Barnaby, A.J. Sprangers, N. Savalia, C.D. James, A. Lee, C.A. Mirkin, A.H. Stegh, Dual bioluminescence and near-infrared fluorescence monitoring to evaluate spherical nucleic acid nanoconjugate activity in vivo, Proceedings of the National Academy of Sciences of the United States of America 114(16) (2017) 4129-4134.
[200] W. Ho, X.Q. Zhang, X. Xu, Biomaterials in siRNA delivery: a comprehensive review, Advanced healthcare materials 5(21) (2016) 2715-2731.
[201] P. Kumthekar, A. Rademaker, C. Ko, K. Dixit, M.A. Schwartz, A.M. Sonabend, L. Sharp, R.V. Lukas, R. Stupp, C. Horbinski, A phase 0 first-in-human study using NU-0129: A gold base spherical nucleic acid (SNA) nanoconjugate targeting BCL2L12 in recurrent glioblastoma patients, American Society of Clinical Oncology, 2019.
[202] L. Kong, J. Qiu, W. Sun, J. Yang, M. Shen, L. Wang, X. Shi, Multifunctional PEI-entrapped gold nanoparticles enable efficient delivery of therapeutic siRNA into glioblastoma cells, Biomaterials science 5(2) (2017) 258-266.
[203] F.M. Kouri, C. Ritner, A.H. Stegh, miRNA-182 and the regulation of the glioblastoma phenotype-toward miRNA-based precision therapeutics, Cell cycle 14(24) (2015) 3794-3800.
[204] F.M. Kouri, L.A. Hurley, W.L. Daniel, E.S. Day, Y. Hua, L. Hao, C.Y. Peng, T.J. Merkel, M.A. Queisser, C. Ritner, H. Zhang, C.D. James, J.I. Sznajder, L. Chin, D.A. Giljohann, J.A. Kessler, M.E. Peter, C.A. Mirkin, A.H. Stegh, miR-182 integrates apoptosis, growth, and differentiation programs in glioblastoma, Genes & development 29(7) (2015) 732-745.
[205] T. Sasayama, K. Tanaka, E. Kohmura, The Roles of MicroRNAs in Glioblastoma Biology and Biomarker, Neurooncology-Newer Developments, InTech2016.
[206] X. Li, L. Xing, K. Zheng, P. Wei, L. Du, M. Shen, X. Shi, Formation of gold nanostar-coated hollow mesoporous silica for tumor multimodality imaging and photothermal therapy, ACS applied materials & interfaces 9(7) (2017) 5817-5827.
[207] A.J. Cole, V.C. Yang, A.E. David, Cancer theranostics: the rise of targeted magnetic nanoparticles, Trends in biotechnology 29(7) (2011) 323-332.
[208] W. Lu, M.P. Melancon, C. Xiong, Q. Huang, A. Elliott, S. Song, R. Zhang, L.G. Flores, 2nd, J.G. Gelovani, L.V. Wang, G. Ku, R.J. Stafford, C. Li, Effects of photoacoustic imaging and photothermal ablation therapy mediated by targeted hollow gold nanospheres in an orthotopic mouse xenograft model of glioma, Cancer research 71(19) (2011) 6116-6121.
[209] H.-W. Yang, H.-L. Liu, M.-L. Li, I.W. Hsi, C.-T. Fan, C.-Y. Huang, Y.-J. Lu, M.-Y. Hua, H.-Y. Chou, J.-W. Liaw, Magnetic gold-nanorod/PNIPAAmMA nanoparticles for dual magnetic resonance and photoacoustic imaging and targeted photothermal therapy, Biomaterials 34(22) (2013) 5651-5660.
[210] J.P.M. Almeida, E.R. Figueroa, R.A. Drezek, Gold nanoparticle mediated cancer immunotherapy, Nanomedicine: Nanotechnology, Biology and Medicine 10(3) (2014) 503-514.
[211] A.Y. Lin, J.P.M. Almeida, A. Bear, N. Liu, L. Luo, A.E. Foster, R.A. Drezek, Gold nanoparticle delivery of modified CpG stimulates macrophages and inhibits tumor growth for enhanced immunotherapy, PloS one 8(5) (2013).
[212] C.-Y. Tsai, S.-L. Lu, C.-W. Hu, C.-S. Yeh, G.-B. Lee, H.-Y. Lei, Size-dependent attenuation of TLR9 signaling by gold nanoparticles in macrophages, The Journal of Immunology 188(1) (2012) 68-76.

[213] G.F. Paciotti, L. Myer, D. Weinreich, D. Goia, N. Pavel, R.E. McLaughlin, L. Tamarkin, Colloidal gold: a novel nanoparticle vector for tumor directed drug delivery, Drug delivery 11(3) (2004) 169-183.
[214] S.K. Libutti, G.F. Paciotti, A.A. Byrnes, H.R. Alexander, W.E. Gannon, M. Walker, G.D. Seidel, N. Yuldasheva, L. Tamarkin, Phase I and pharmacokinetic studies of CYT-6091, a novel PEGylated colloidal gold-rhTNF nanomedicine, Clinical cancer research 16(24) (2010) 6139-6149.
[215] Y. Liu, P. Chongsathidkiet, B.M. Crawford, R. Odion, C.A. Dechant, H.R. Kemeny, X. Cui, P.F. Maccarini, C.D. Lascola, P.E. Fecci, Plasmonic gold nanostar-mediated photothermal immunotherapy for brain tumor ablation and immunologic memory, Immunotherapy 11(15) (2019) 1293-1302.
[216] S. Ruan, R. Xie, L. Qin, M. Yu, W. Xiao, C. Hu, W. Yu, Z. Qian, L. Ouyang, Q. He, Aggregable nanoparticles-enabled chemotherapy and autophagy inhibition combined with anti-PD-L1 antibody for improved glioma treatment, Nano letters 19(11) (2019) 8318-8332.
[217] M.M. Janát-Amsbury, A. Ray, C.M. Peterson, H. Ghandehari, Geometry and surface characteristics of gold nanoparticles influence their biodistribution and uptake by macrophages, European Journal of Pharmaceutics and Biopharmaceutics 77(3) (2011) 417-423.
[218] K. Niikura, T. Matsunaga, T. Suzuki, S. Kobayashi, H. Yamaguchi, Y. Orba, A. Kawaguchi, H. Hasegawa, K. Kajino, T. Ninomiya, Gold nanoparticles as a vaccine platform: influence of size and shape on immunological responses in vitro and in vivo, ACS nano 7(5) (2013) 3926-3938.
[219] S. Salatin, S. Maleki Dizaj, A. Yari Khosroushahi, Effect of the surface modification, size, and shape on cellular uptake of nanoparticles, Cell biology international 39(8) (2015) 881-890.
[220] K.C.L. Black, Y. Wang, H.P. Luehmann, X. Cai, W. Xing, B. Pang, Y. Zhao, C.S. Cutler, L.V. Wang, Y. Liu, Radioactive 198Au-doped nanostructures with different shapes for in vivo analyses of their biodistribution, tumor uptake, and intratumoral distribution, ACS nano 8(5) (2014) 4385-4394.
[221] Y. Liu, Z. Wang, Y. Liu, G. Zhu, O. Jacobson, X. Fu, R. Bai, X. Lin, N. Lu, X. Yang, Suppressing Nanoparticle-Mononuclear Phagocyte System Interactions of Two-Dimensional Gold Nanorings for Improved Tumor Accumulation and Photothermal Ablation of Tumors, ACS nano 11(10) (2017) 10539-10548.
[222] B. Zhang, T. Lan, X. Huang, C. Dong, J. Ren, Sensitive single particle method for characterizing rapid rotational and translational diffusion and aspect ratio of anisotropic nanoparticles and its application in immunoassays, Analytical Chemistry 85(20) (2013) 9433-9438.
[223] P. Puvanakrishnan, J. Park, D. Chatterjee, S. Krishnan, J.W. Tunnell, In vivo tumor targeting of gold nanoparticles: effect of particle type and dosing strategy, International journal of nanomedicine 7 (2012) 1251-1258.
[224] Y. Liu, W. Lu, Recent advances in brain tumor-targeted nano-drug delivery systems, Expert opinion on drug delivery 9(6) (2012) 671-686.
[225] O. Van Tellingen, B. Yetkin-Arik, M. De Gooijer, P. Wesseling, T. Wurdinger, H. De Vries, Overcoming the blood–brain tumor barrier for effective glioblastoma treatment, Drug Resistance Updates 19 (2015) 1-12.
[226] R.W. Chakroun, P. Zhang, R. Lin, P. Schiapparelli, A. Quinones-Hinojosa, H. Cui, Nanotherapeutic systems for local treatment of brain tumors, Wiley Interdisciplinary Reviews: Nanomedicine and Nanobiotechnology 10(1) (2018) e1479.
[227] L.P. Ganipineni, F. Danhier, V. Préat, Drug delivery challenges and future of chemotherapeutic nanomedicine for glioblastoma treatment, Journal of controlled release 281 (2018) 42-57.
[228] F. Danhier, To exploit the tumor microenvironment: Since the EPR effect fails in the clinic, what is the future of nanomedicine?, Journal of Controlled Release 244 (2016) 108-121.
[229] N. Schleich, F. Danhier, V. Préat, Iron oxide-loaded nanotheranostics: major obstacles to in vivo studies and clinical translation, Journal of Controlled Release 198 (2015) 35-54.

[230] F. Zhang, P. Mastorakos, M.K. Mishra, A. Mangraviti, L. Hwang, J. Zhou, J. Hanes, H. Brem, A. Olivi, B. Tyler, Uniform brain tumor distribution and tumor associated macrophage targeting of systemically administered dendrimers, Biomaterials 52 (2015) 507-516.
[231] Y. Zhu, J. Feijen, Z. Zhong, Dual-targeted nanomedicines for enhanced tumor treatment, Nano Today 18 (2018) 65-85.
[232] J. Wolfram, M. Ferrari, Clinical cancer nanomedicine, Nano Today (2019).
[233] X. Gao, Q. Yue, Z. Liu, M. Ke, X. Zhou, S. Li, J. Zhang, R. Zhang, L. Chen, Y. Mao, Guiding Brain-Tumor Surgery via Blood–Brain-Barrier-Permeable Gold Nanoprobes with Acid-Triggered MRI/SERRS Signals, Advanced Materials 29(21) (2017) 1603917.
[234] F. Burgio, D. Piffaretti, F. Schmidt, U. Pieles, M. Reinert, M.-F. Ritz, S.S. Saxer, Tuning the surface chemistry of gold nanoparticles to specifically image glioblastoma cells using surface-enhanced Raman spectroscopy, ACS Applied Nano Materials (2020).
[235] R. Komeri, B. Unnikrishnan, J. Sreekutty, P. GU, K.K. Maiti, T.T. Sreelekha, Galactoxyloglucan-Modified Gold Nanocarrier of Doxorubicin for Treating Drug-Resistant Brain Tumors, ACS Applied Nano Materials 2(10) (2019) 6287-6299.
[236] A. Orza, O. Soriţău, C. Tomuleasa, L. Olenic, A. Florea, O. Pana, I. Bratu, E. Pall, S. Florian, D. Casciano, Reversing chemoresistance of malignant glioma stem cells using gold nanoparticles, International journal of nanomedicine 8 (2013) 689.
[237] A. Kefayat, F. Ghahremani, H. Motaghi, A. Amouheidari, Ultra-small but ultra-effective: Folic acid-targeted gold nanoclusters for enhancement of intracranial glioma tumors' radiation therapy efficacy, Nanomedicine: Nanotechnology, Biology and Medicine 16 (2019) 173-184.
[238] B. Seo, K. Lim, S.S. Kim, K.T. Oh, E.S. Lee, H.-G. Choi, B.S. Shin, Y.S. Youn, Small gold nanorods-loaded hybrid albumin nanoparticles with high photothermal efficacy for tumor ablation, Colloids and Surfaces B: Biointerfaces 179 (2019) 340-351.
[239] D. Gonçalves, D. Park, T. Schmidt, C. Werner, Modular peptide-functionalized gold nanorods for effective glioblastoma multicellular tumor spheroid targeting, Biomaterials science 6(5) (2018) 1140-1146.
[240] G. Battogtokh, O. Gotov, J.H. Kang, E.J. Hong, M.S. Shim, D. Shin, Y.T. Ko, Glycol chitosan-coated near-infrared photosensitizer-encapsulated gold nanocages for glioblastoma phototherapy, Nanomedicine: Nanotechnology, Biology and Medicine (2018).
[241] Q. Lu, X. Dai, P. Zhang, X. Tan, Y. Zhong, C. Yao, M. Song, G. Song, Z. Zhang, G. Peng, Fe3O4@ Au composite magnetic nanoparticles modified with cetuximab for targeted magneto-photothermal therapy of glioma cells, International journal of nanomedicine 13 (2018) 2491.
[242] L. Zhao, Y. Li, J. Zhu, N. Sun, N. Song, Y. Xing, H. Huang, J. Zhao, Chlorotoxin peptide-functionalized polyethylenimine-entrapped gold nanoparticles for glioma SPECT/CT imaging and radionuclide therapy, Journal of nanobiotechnology 17(1) (2019) 30.
[243] L. Li, Y. Liu, J. Yang, Q. Zhang, M. Lu, X. Wang, L. Li, L. Ren, Targeted Combination Therapy for Glioblastoma by Co-Delivery of Doxorubicin, YAP-siRNA and Gold Nanorods, YAP-siRNA and Gold Nanorods (July 10, 2019) (2019).

Figure Legends

Fig. 1. Theranostic applications of AuNPs in various cancers

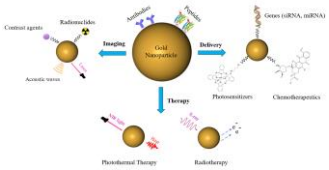

Fig. 2. A) Two-dimensional axial MRI, photoacoustic and Raman images for detection of brain tumors in living mice; B) Raman-guided intraoperative surgery. When the entire tumor was removed visually, several small foci of Raman signals were found in the resection bed. Adapted from Ref [14] with permission.

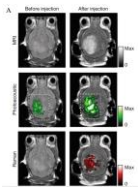

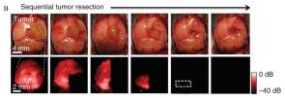

Fig. 3. A) T2W-MR images of mouse brain bearing U87-EGFRvIII+ glioblastoma xenograft before and at selected time points post-injection (PI) of AuP-FAL (upper panel) or AuP-PEG (lower panel) via i.v. (0.05 mmol kg−1 [Gd3+]). B) Histologic H&E images of the identical mouse brains presented in panel A. C) Color-coded ΔT1-map of mouse brains at 24 h post-injection of AuP-FAL or AuP-PEG. Arrows indicate the tumor. D) Time-dependent T1 value of the brain tumor (black line) and contralateral normal brain tissue (gray line) before and at selected time points post-injection of the nanoprobe. At 1 h PI, AuP-FAL led to a 13.3% (pre-injection vs. post-injection, P = 0.099) T1 value reduction in the tumor area, which is significantly higher than the value of 8.7% (P = 0.139) after AuP-PEG injection. At 24 h PI, AuP-FAL led to 14.8% (P = 0.022) T1 value reduction in the tumor area, which is also significantly higher than the value of AuP-PEG (10%, P = 0.113). AuP: Au Nanoprobes; cc: color-coded. Adapted from Ref [98] with permission.

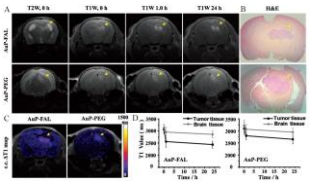

Fig. 4. A) *In vivo* fluorescence images of U87MG tumor-bearing nude mice at various time points following injection of Cy7-labeled cRGD-HNs or HNs; B) DOX fluorescence images of tumors and organs 8 h post-injection of cRGD-HN-DOX and HN-DOX in U87MG glioma bearing nude mice; C) quantification of DOX accumulated in different organs and tumors using fluorescence spectroscopy (n=3). Adapted from Ref [65] with permission.

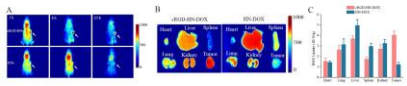

Fig. 5. A) Photograph of a tumor-bearing mouse under PTT. PEGylated nanocages or saline was i.v. injected. The inset shows a TEM image of the Au nanocages with an edge length of 48±3.5 nm. After 72 h in which nanocages were cleared from the circulation, the tumor on the right flank was irradiated by the diode laser (0.7W cm-2); B–G) thermographic images of B–E) nanocage-injected and F–I) saline-injected tumor-bearing mice at various time points: B, E) 1 min, C, F) 3 min, D, G) 5 min, and E, I) 10 min. J) Plots of average temperature within the tumors as a function of irradiation time. Scale bars are 1 cm. Adapted from Ref [58] with permission.

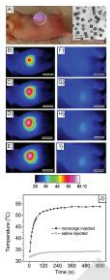

Fig. 6. (1) Side flank tumor xenograft model. A) scheme of RVG peptide-PEG5k-conjugated AuNRs coated with SiO2 (RVG-PEG-AuNRs@SiO2); B) *In vivo* fluorescence images of RVG-PEG-AuNRs@SiO2, RVGPEG- AuNPs@SiO2, PEG-AuNRs@SiO2, and PEG-AuNPs@SiO2 in orthotopic glioma-bearing mice at various time points (2, 4, 8, 24 h) after i.v injections; C) Representative images of N2a cells-xenografted mice treated with saline, PEGAuNRs@SiO2, RVG-PEG-AuNRs@SiO2 at days 0, 1, 3, 7, 10, and 13 d after NIR laser irradiation (808 nm, 1.5 W cm−2, 5 min); D) Images of tumors

excised from mice treated with (a,b) saline, (c,d) PEG-AuNRs@SiO2, (e,f) RVG-PEG-AuNRs@SiO2 with or without NIR laser irradiation, respectively; E) Tumor volumes of mice treated with RVG-PEG-AuNRs@SiO2, PEG-AuNRs@SiO2 with or without NIR laser irradiation: *P < 0.001 over PEG-AuNRs@SiO2 (NIR+); **P < 0.003 over PEG-AuNRs@SiO2 (NIR+); ***P < 0.004 over saline (NIR+). (2) Orthotopic brain tumor model. MRI images of brains of orthotopic N2a glioma-bearing mice treated with (a) saline, (b) PEG-AuNRs@SiO2, or (c) RVG-PEG-AuNRs@SiO2 with NIR laser irradiation. Adapted from Ref [171] with permission.

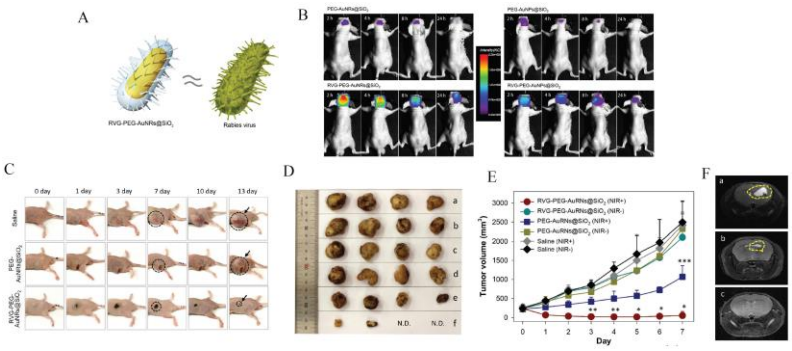

Fig. 7. Scheme of PDT resistance mechanism. Nrf2, the key transcription factor in a self-adapting system, is detached from Kelch-like ECH-associated protein 1 (KEAP1) in cytoplasm under an oxidative condition (PDT) and then is transferred to nucleus, that activates transcription of various downstream target genes encoding resistance-related transport proteins (such as ABCG2), antioxidant proteins (such as NQO-1) and environment-response proteins (such as HIF-1α). Adapted from Ref [74] with permission.

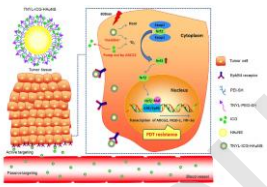

Table 1. Paradigmatic applications of gold nanoparticles in glioma theranostic

Application	Nanoparticle	Active component	Targeting component	Size (nm)	Highlight	Ref
Imaging	Au-silica core-shell NP	trans-1,2-bis(4-pyridyl)-ethylene; DOTA-Gd	-	~120	This platform used for triple-modality of MRI-PA-Raman imaging for both pre- and intra-operatively, facilitating removal small tumor foci.	[14]
	PEG-AuNS	IR783B; DTPA-Gd	FAL peptide	60	This platform used for MRI and intra-operatively guiding resection by SERRS imaging.	[98]
	PEG-AuNS	IR783B; DTPA-Gd	Angiopep-2	D_H: 25	Removal of acid-labile PEG shielding layer in an acidic tumor environment exposed the azide and alkyne moieties on Au surface, facilitating click cycloaddition and aggregation with the concomitant activation of both MRI and SERRS signals.	[233]
	PEG-AuNP	1,4-BDT	anti-EGFR	D_H: <90	The Raman reporter, 1,4-BDT, was immobilized on AuNP surface for maximal SERS sensitivity.	[234]
	PEG-AuNR	^{64}Cu	RGD	50×15	chelator-free ^{64}Cu radiolabeling via chemically reducing ^{64}Cu on the surface of RGD-PEG-AuNR for PET imaging.	[103]
Chemotherapy	PEG- AuNP	DOX	Angiopep-2	~40	DOX was attached to AuNPs via hydrazine, acid-responsive, linker, while angiopep-2 mediated NPs uptake via interaction with LRP1.	[67]
	PEG–PCL/AuNR	DOX	cRGD	50×15	DOX's release was accelerated by NIR irradiation, and the cRGD-DOX-NPs + NIR could completely inhibit tumor growth in U87MG tumor-bearing mice, which was more effective than free DOX.	[65]
	Gelatin-AuNP	DOX	RRGD	D_H: 188	NPs showed size-shrinkage effect (188 nm to 56 nm) via digestion of gelatin by MMP-2, overexpressed in tumors. DOX was attached to AuNPs via hydrazone bond enabling a pH-triggered release (14% and 91.9%, at pH 7.4 and 5.0 respectively at 48 h).	[113]
	PAA-AuNP	Cisplatin	Uptake peptide (PKKKRKV)	7	FUS enhanced BBB permeability and delivery of cisplatin conjugated to AuNPs	[120]
	AuNP	DOX	Galactoxyloglucan	D_H<100	AuNPs were capped with galactoxyloglucan (PST001), which can selectively bind tumor necrosis factor-related apoptosis-inducing ligand (TRAIL) overexpressed on some types of cancer cells.	[235]
	PEG-AuNP	DOX, HCQ	-	~ 45	Using various coatings, legumain-responsive PEG-AuNPs were prepared, enabling *in situ* aggregate formation in response to overexpressed legumain, resulting in enhanced accumulation of DOX and HCQ. Co-administration of	[216]

					AuNPs with anti-PD-L1 antibody could induce memory immunity, preventing glioma recurrence.	
	L-aspartate-AuNP	TMZ	-	55	The NP-TMZ was found more effective in apoptosis induction in glioma-derived cancer stem cells.	[236]
Radiotherapy	PEG-AuNP	-	-	D: 12 D_H: 23	RT increased the accumulation of AuNPs in tumor through enhancing BBB permeability, and the mice receiving AuNPs plus RT showed a median survival of 28 days vs 14 days for RT alone.	[30]
	BSA-AuNP	-	-	D:18 D_H: 28	NPs plus RT enhanced DNA double-strand break and cell apoptosis compared to RT alone in U87 cells.	[28]
	Coated AuNP (AuroVist™)	-	-	11	NPs enhanced local radiation dose by approximately 300% *in vivo.*	[44]
	BSA -AuNC	-	Folic acid	D_H: 5.5	Such NPs showed a dose enhancement factor of 1.6 upon RT, as well as enhanced survival compared to RT alone, in glioma-bearing rats.	[237]
Photothermal Therapy	PEG-Au-silica core-shell NP	-	-	152	The NPs plus laser irradiation showed complete tumor regression with overall survival of 57% for 90 days, while in mice received laser irradiation alone, tumors progressed rapidly with a mean survival of 13.3 days.	[167]
	PEG-Au nanocage	-	-	D: 48 D_H: 92	Upon laser irradiation, in NP-injected mice, the tumor surface temperature increased rapidly to 50 °C, while in saline-injected mice, the surface temperature remained below 37°C.	[58]
	AuNR-loaded albumin-NP	-	-	20.5 ×4.6	Albumin NPs was found effective in carrying AuNRs into N2a tumors *in vivo*, and enhanced tumor targeting compared to naïve AuNRs.	[238]
	PEG-Au-silica core-shell NP	-	anti-HER2, anti-IL13Ra2	110	Anti-HER2 tagged NPs induced cell death in medulloblastoma cell expressing HER2, and anti-IL-13Ra2 tagged NPs exhibited cell death in glioma cells (U87 and U373) expressing IL-13Ra2, upon laser irradiation.	[72]
	PEG-silica-AuNRs	-	RVG	120×50	The i.v. injected RVG-PEG-SiO_2-AuNRs showed a higher localization in the brain region of mice than did the spherical nanoparticles.	[171]
	PEG-AuNR	-	Nestin-binding peptide	28×9	Such NPs could target solid tumors originated from human GBM cancer stem cells, expressing Nestin on their surface.	[239]
Photodynamic Therapy	PEG-AuNP	Pc 4	-	D: 5 D_H: 38	Faster drug accumulation to the target tumor compared to free Pc4 (≤6 h for Pc 4-AuNPs vs ~48 h for fee Pc 4).	[180]
	PEG-AuNP	Pc 4	Tf_{pep}	D:5 D_H: 12	Tf_{pep}-Pc 4-Au augmented drug accumulation by 6 ± 2.2-fold in the brain of orthotopic U87-bearing mice, compared to untargeted Pc 4-Au.	[68]

	PEG-AuNP	Pc 4	EGF_{pep}	5	EGF_{pep}-AuNP-Pc 4 enhanced the delivery of Pc 4 to the subcutaneous glioma tumor in mice by 3.3-fold compared to AuNP-Pc 4.	[70]
	PEG-AuNP	Pc 4	EGF_{pep}, Tf_{pep}	D: 5 D_H: 41	Dual-targeted (EGF_{pep}+Tf_{pep})-AuNPs-Pc 4 showed significant improvement in drug uptake and cell killing compared to single-targeted formulations.	[181]
	PEG-PEI-AuNS (hallow)	ICG	TNYL peptide	50	TNYL-ICG-HAuNS could overcome the PDT resistance of cancer cells caused upon exposure to ICG.	[74]
	GC-Au nanocage	SiNC	-	D_H: 160	Nanocage was coated with GC through an enzyme-cleavable peptide linkage that could be detached in the presence of cathepsin B enzyme, enabling SiNC release in the cytoplasm.	[240]
Gene Therapy	PEG-AuNP	Bcl2L12-specific siRNA	-	13	The NPs-siRNA decreased Bcl2L12 expression in intracerebral GBM tumor, enhanced apoptosis, and reduced tumor burden and progression *in vivo.*	[182]
	PEI-PEG-AuNP	Bcl-2 siRNA	RGD	2.9	-	[202]
	PEG-AuNP	MiR-182	-	13 nm	AuNPs-miR-182 could reduce tumor burden and increased survival of glioma-bearing mice.	[204]
	DSPEI-AuNR	Small hairpin RNA (shRNA)	RGD	50 × 10	Combining the capabilities of: passive and active targeting (via $\alpha_v\beta_3$ integrin-mediated endocytosis), intracellular glutathione-triggered ‘‘off–on’’ release (via cross-linking disulfide bonds to unpack PEI shell) and endosomal escape (via PEI).	[196]
Multimodal Regimens	PNIPAAmMA-AuNR-Fe_3O_4 conjugated NP	-	-	60.6 × 10.4	MRI and PA imaging besides PTT. A Temperature rise by 62 °C upon irradiation due to the high concentration of magnetic NRs under a magnetic field.	[209]
	Au-Fe_3O_4 core-shell NP	-	Cetuximab	D_H: 46	Such NPs were utilized in combined magnetic hyperthermia and NIR PTT.	[241]
	PEG-AuNS (hallow NS)	-	cRGD	40	Targeted PA imaging and PTT.	[208]
	PEI-AuNP	^{131}I	Chlorotoxin peptide	D_H: 151	Nanoprobe for targeted SPECT/CT imaging and radionuclide therapy of glioma cells.	[242]
	PEG-AuNP	DOX and Gd^{3+}	TAT	D: 4.7 D_H:21.4	Prolonged retention time of Gd^{3+} compared to free Gd^{3+} chelates *in vivo*.	[19]
	Liposomes loaded with AuNRs	DOX YAP-siRNA	Angiopep-2	Liposome D: 120 AuNR 80×15	The combination of chemotherapy, gene therapy and PTT was found synergistically effective to prolong the survival time of GBM-bearing mice.	[243]

1,4-BDT: 1,4-Benzenedithiol AuNC: Au nanocluster; AuNR: Au nanorod; AuNS: Au nanosphere; DSPEI: disulfide cross-linked PEI; DTPA: Diethylenetriaminepentaacetic acid; EGFpep: epidermal growth factor peptide; FAL peptide: (Phe-Ala-Leu-Gly-Glu-Ala) as an EGFRvIII targeting ligand; GC: Glycol chitosan; HCQ: hydroxychloroquine; IL13Ra2: interleukin-13 receptor alpha 2; LRP1: lipoprotein receptor-related protein-1;

PAA: polyacrylic acid; Pc 4: Silicon phthalocyanine 4; PEI: polyethyleneimine; RVG: rabies virus glycoprotein; SERRS: surface-enhanced resonance Raman scattering; SiNC: silicon 2,3-naphthalocyanine bis (trihexylsilyloxide); TMZ: temozolomide; YAP: yes-associated protein.